GEOMORPHIC ANALYSIS OF A LATE PLEISTOCENE LAKE BONNEVILLE SPIT COMPLEX, DEEP CREEK MOUNTAINS, UTAH

by

Paul Matthew Thomas

A thesis submitted to the faculty of
The University of Utah
in partial fulfillment of the requirements for the degree of

Master of Science

in

Geology

Department of Geology and Geophysics

The University of Utah

August 2014

The University of Utah Graduate School

STATEMENT OF THESIS APPROVAL

The following faculty members served as the supervisory committee chair and members for the thesis of **Paul Matthew Thomas**.

Dates at right indicate the members' approval of the thesis.

Paul W. Jewell, Chair	**6/4/2014**	Date Approved
Holly S. Godsey, Member	**6/4/2014**	Date Approved
Jeffrey R. Moore, Member	**6/4/2014**	Date Approved

The thesis has also been approved by **John M. Bartley**

Chair of the Department/School/College of **Geology and Geophysics**

and by David B. Kieda, Dean of The Graduate School.

ABSTRACT

The Deep Creek Mountains, located on the border of Utah and Nevada, are part of Late Pleistocene Lake Bonneville's western boundary and are relatively undocumented in terms of Quaternary stratigraphy and geomorphology. This mountain range offers a unique opportunity to study the interactions of alluvial systems before, during, and after the presence of Lake Bonneville. Preserved along the range, at the base of Reilly Wash, is a large barrier complex with spit-bar elements, as well as "intermediate shorelines" or embankments, as described and puzzled over by G.K. Gilbert more than 120 years ago.

This study focuses on mapping one of the largest barrier complexes in the Bonneville basin and reevaluates Gilbert's brief geomorphologic and sedimentologic assessments using modern techniques. The significance of these intermediate shoreline features, which can be found primarily between the Stansbury, Bonneville, and Provo shorelines, are described by reconstructing the transgressive and regressive states of Lake Bonneville in this portion of the basin through observing a number of geomorphic features and sediment exposures. These include bedded marls, well-preserved regressive Provo sediments representing waning post-Bonneville flood stages, and a boulder strandline marking the transition from alluvial fan material to Bonneville sediments. Nine new radiocarbon accelerator mass spectrometry analyses from *in situ* gastropods provide dates to bracket the depositional chronology of the complex, from

~20,000 ^{14}C yr B.P. to the Bonneville Flood (~14,500 ^{14}C yr B.P.), and support the hypothesis that links intermediate shoreline deposition to lake oscillations (Unnamed 2 and Unnamed 3).

Fluvial modeling and tectonic geomorphic analyses were used to determine the approximate age of the alluvial fan deposition from which the spit complex extends and to estimate the volume of the complex. Tectonic geomorphic indices, mountain front sinuosity (Smf), valley floor width-to-height ratio (Vf) and hypsometric integral (HI) highlight the watersheds in the vicinity of the spit complex as being the least developed in the range in terms of watershed maturity. This immaturity is believed to be cause by previously undocumented tectonic activity near these watersheds, depositing two large alluvial fans, in the mid-late Quaternary. Volumetric estimates conclude that the spit complex is ~75 million cubic meters, which is 2 to 3 times larger than the Stockton Bar, a landform that was previously thought to be one of the largest barrier bars formed in Lake Bonneville. This study is the first modern exploration of the interaction of Lake Bonneville and the Deep Creek Mountains. Future work documenting the depositional chronology of other landforms along the range is needed before a correlation of intermediate shorelines can be made.

TABLE OF CONTENTS

APPENDICES

LIST OF FIGURES

LIST OF TABLES

ACKNOWLEDGEMENTS

I would like to thank my advisor Paul Jewell for his insight over the duration of this project along with my committee, Holly Godsey and Jeffrey Moore. Heaps of thanks to the best field assistant a person could ask for, Alex Lowe. Along with friends and family, thank you for your support and words of encouragement, it got me to where I am today.

INTRODUCTION

Purpose of Study

Late Pleistocene Lake Bonneville is an ideal locality for lacustrine environmental and paleoclimate analyses due to the well-preserved nature and wide variety of landforms throughout the basin. Geomorphic, hydrodynamic, and sedimentologic interpretations of these lacustrine landforms have led to the development of detailed models used to simulate climate patterns during the transgression and regression of the largest pluvial lake in the Late Pleistocene (Gilbert, 1890; Currey and Oviatt, 1985; Oviatt et al., 1992; Jewell, 2007). This study represents a thorough field examination of a large spit complex, its adjoining mountain range, and the subsequent paleo-geomorphic information gathered from field and computational investigations.

The Deep Creek Range is located on the border of Utah and Nevada on the western edge of the Bonneville basin (Figure 1) and is relatively undocumented in terms of Quaternary stratigraphy and geomorphology. This region offers a unique opportunity to study the interactions of alluvial systems before, during, and after the presence of Lake Bonneville due to lack of anthropogenic impacts along the Deep Creeks, compared to the heavily modified landforms of the Wasatch Front. This study focuses on the geomorphologic and sedimentologic features of the spit-bar complex, hereafter known as Reilly Wash Spit Complex (RWSC), to create a detailed depositional history and

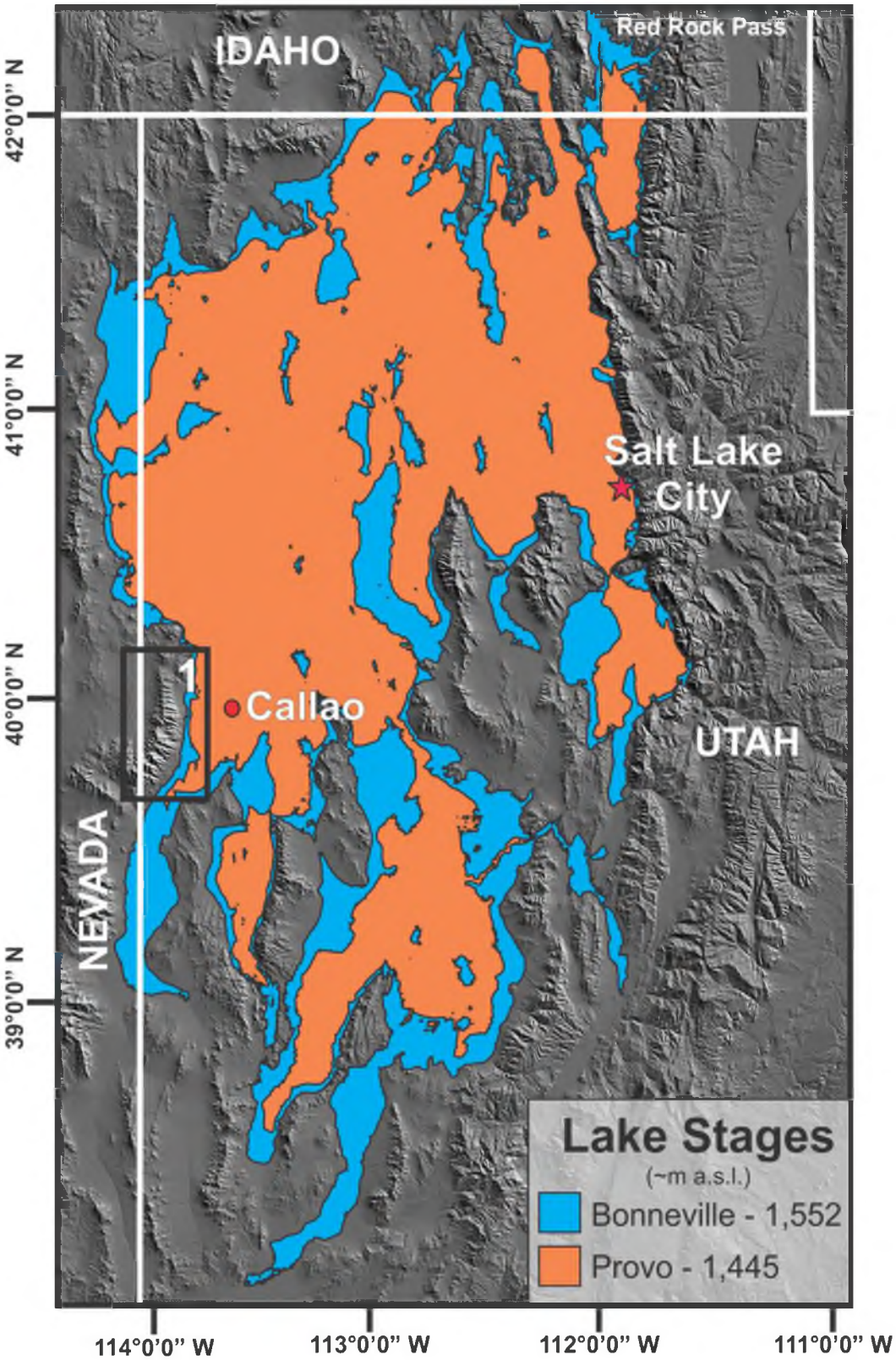

Figure 1. Map of Lake Bonneville at two lake elevations (Bonneville and Provo). Documented lake elevations are corrected for isostatic rebound. Box 1 indicates the location of the study area, Deep Creek Mountains (Figure 2).

hydrodynamic model that can be put into context of the rest of the Bonneville basin and possible transgressive oscillations of the lake (Oviatt, 1997; Benson, 2011). This is accompanied by an investigation of relative tectonic activity using geomorphic indices and an analysis of the Deep Creek watershed (Figure 2) to investigate the depositional origin of the alluvial fan, which has been interpreted to be the spit complex's sediment source.

Lake Bonneville

Lake Bonneville was primarily a closed-basin lake that covered much of present day Utah, eastern Nevada, and southern Idaho (Figure 1) that, at its maximum, had an area of 51,500 km^2 and a depth of approximately 300 meters. The initial transgression of Lake Bonneville in the basin began around 28,000 ^{14}C yr B.P (Figure 3). This transgressive phase continued until the lake reached its maximum elevation of approximately 1,552 meters above sea level (m a.s.l.), approximately 15,500 ^{14}C yr B.P. (Oviatt, 1997).

During the transgressive phase of Lake Bonneville, movement of the Polar Jet Stream (PJS) over the Great Basin resulted in a change in regional climate (Oviatt, 1997; Benson, 2011). It is hypothesized that these shifts in climate resulted in oscillations to the pluvial lake, as it was sensitive to water input from precipitation and glacial ice extents (Jewell, 2007). Oviatt (1997) documents these lake level oscillations (Figure 3) at approximately 22-20 ^{14}C ka (Stansbury oscillation), 18.5-19 ^{14}C ka (Unnamed Oscillation 1), 17 ^{14}C ka (Unnamed Oscillation 2), and 15-15.5 ^{14}C ka (Unnamed Oscillation 3).

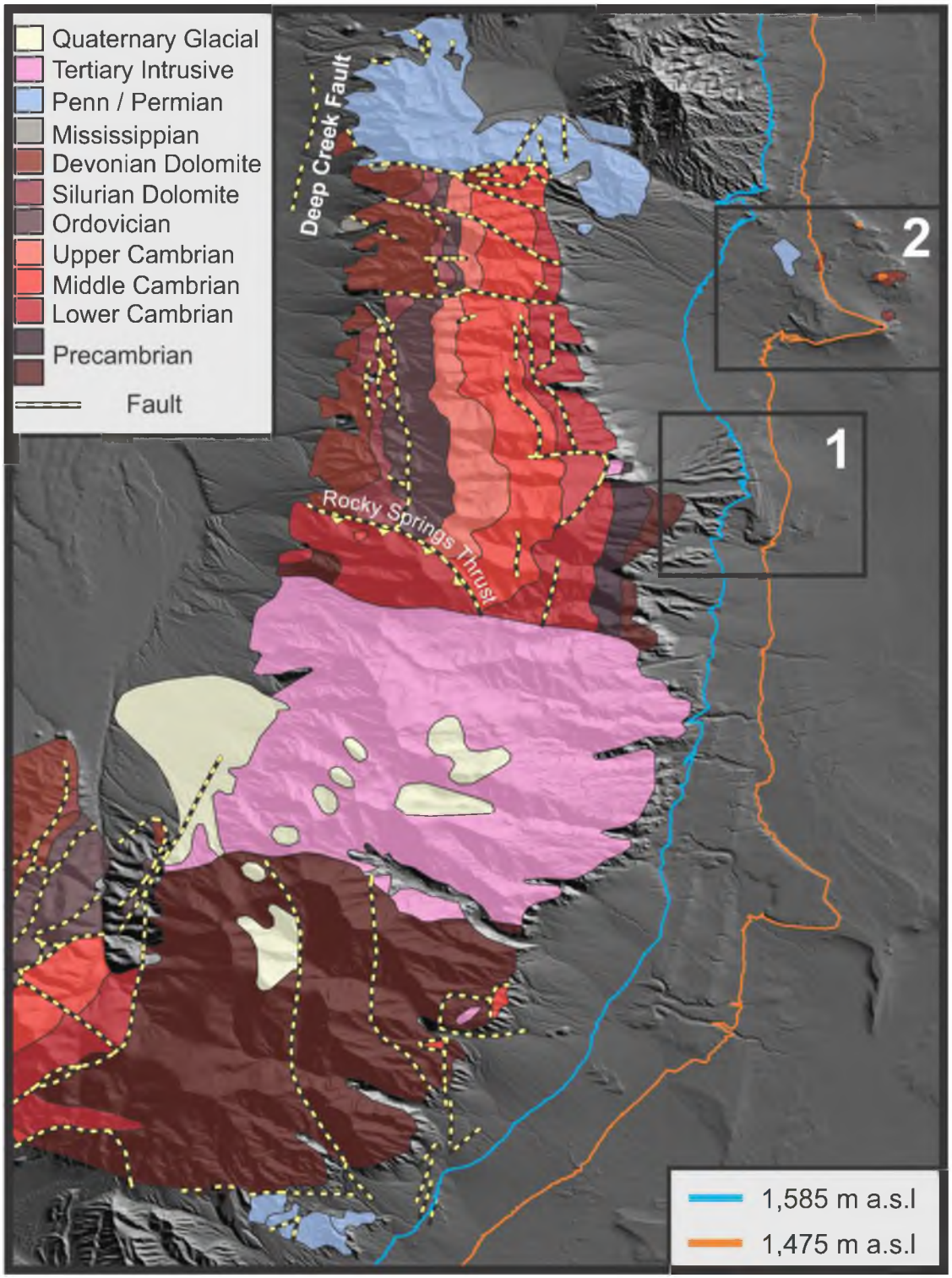

Figure 2. Geologic map of the Deep Creek Mountains, UT. Lake Bonneville's Provo and Bonneville lake elevations have not been adjusted for isostatic rebound. Box 1): Reilly Wash Spit Complex (Figure 5), Box 2): Hook spit and tombolo (Figure 6). Modified from Rodgers (1989) and Hintze et al. (2000).

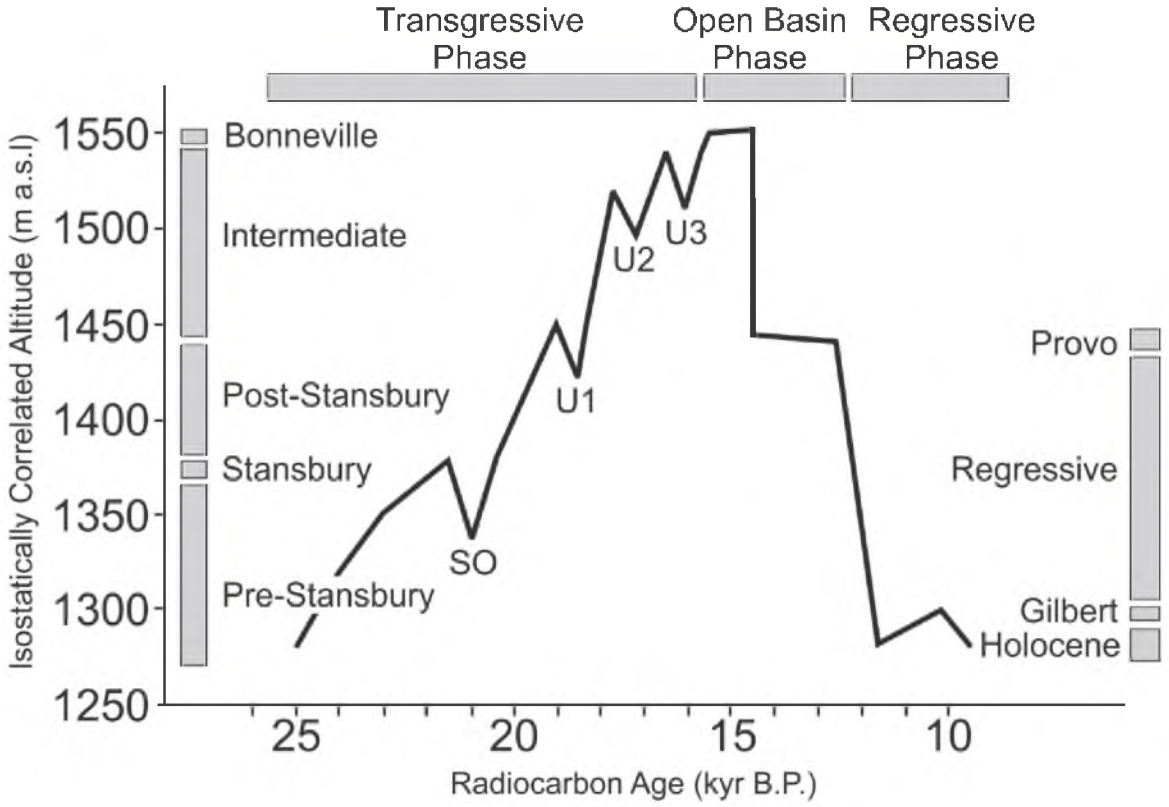

Figure 3. Hydrograph of Lake Bonneville. Vertical boxes correlate to different stages of Lake Bonneville. Horizontal boxes represent the three phases of Lake Bonneville (Gilbert, 1890). SO – Stansbury Oscillation, U1 – Unnamed oscillation 1, U2 – Unnamed oscillation 2, U3 – Unnamed oscillation 3 (Oviatt, 1997). Elevations corrected for isostatic rebound (Oviatt, 1992). Figure modified from Nelson (2012).

Transgression of the lake ended when waters began to overflow at the Zenda, Idaho threshold, an unconsolidated natural alluvial dam, near Red Rock Pass, Idaho (Figure 1). The ensuing catastrophic failure of these alluvial materials (~14,500 ^{14}C yr B.P.) caused lake waters to flood into the Snake River drainage to the north (Oviatt, 1992; O'Connor, 1993; Janecke, 2011). The Bonneville flood lasted as much as one year and drained ~4,700 km^3 of water into the Snake River and Columbia River drainages with a peak discharge rate of 10^6 m^3/s (O'Connor, 1993). The flood is considered to be the largest lake-dam failure of the Quaternary and left numerous geomorphic markers (boulder strands marking high water levels, excavated and rounded volcanic boulders, and numerous gravel deposits) that have been used to calculate discharge and timing (O'Connor, 1993; O'Connor, 2004; Janecke, 2011).

Following the Bonneville flood, the lake level dropped ~108 meters from the Bonneville highstand and continued to overflow at a new topographic divide located southwest of Red Rock Pass, Idaho (Gilbert, 1890; Malde, 1968; Currey et al., 1985). Lake level stabilized at an elevation of approximately 1,445 meters, referred to as the Provo stage, until a shift in climate approximately 12,500 ^{14}C yr B.P. caused the lake to permanently drop below the threshold, marking the transition from an open to closed lake basin (Oviatt et al., 1990; Oviatt, 1992; O'Connor, 1993; Godsey, 2011). The lake continued to regress, with the exception of a slight transgression around 10,000 ^{14}C yr B.P. that formed the Gilbert shoreline, before reaching the modern day Great Salt Lake elevation (Oviatt et al., 2005).

Lake Bonneville has been of interest to researchers for over 120 years due to the well-defined and well-preserved shore platforms and associated lacustrine landforms. G.K. Gilbert, a prominent figure in the U.S. Geological Survey, was one of the first scientists to travel throughout the lake basin. He described the lacustrine system and associated impacts of isostasy, and attempted to correlate major and minor shorelines. Gilbert also studied sediment transport and the role of fetch and wave energy in the construction of the numerous large landforms in the basin. His detailed notebooks and 1890 monograph depict these features and the timing of their deposition in the form of a basic hydrograph (Gilbert, 1890; Hunt, 1981).

One aspect of Lake Bonneville that puzzled Gilbert and subsequent researchers is the depositional chronology and a lack of correlation of "intermediate embankments," referred to here as intermediate shorelines (Figure 4). Although the exact depositional or erosional nature of these shorelines has not been determined, they are of interest due to the possibility that they may represent oscillations of Lake Bonneville that reflect global or regional climatic shifts.

G. K. Gilbert (1890) had numerous hypotheses regarding the nature of these intermediate shorelines and concluded that most, if not all, of these features were formed during the transgression of the lake. Most perplexing to him was lack of correlation between altitudes of these intermediate embankments with various landforms throughout the basin. Though there is mention of the Deep Creek Range and the associated spit complex in his monograph, he

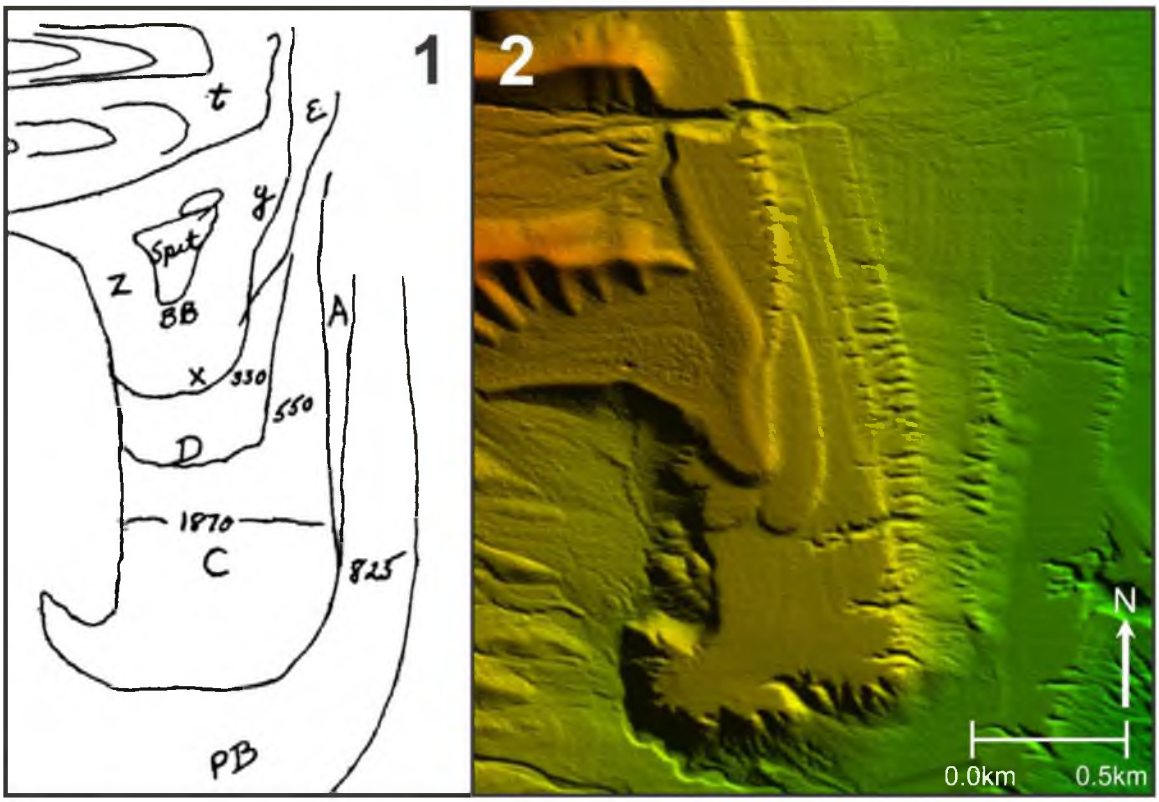

Figure 4. Comparison of field sketch and digital elevation map of Reilly Wash Spit Complex.1) G.K. Gilbert sketch modified from (Hunt, 1981). Lettered shorelines A, C, D, and E refer to intermediate shorelines, PB – Provo shoreline, and BB – Bonneville shoreline. 2) 5-meter hill-shaded digital elevation map of Reilly Wash Spit Complex.

published nothing more than a sketch and brief description of the area (Gilbert, 1890; Hunt, 1981). As one of the largest spits in the Bonneville basin, and having well-preserved intermediate shorelines, the Reilly Wash Spit Complex is an excellent site to reevaluate Gilbert's geomorphologic and sedimentologic assessment of the area using modern techniques. This study uses computer-generated digital elevation models and radiocarbon dating to bracket the depositional chronology and mechanisms of these intermediate shorelines and their relation to possible oscillations during the transgression of Lake Bonneville.

Field Locality

The Deep Creek Range (Figure 2), located in the Basin and Range Province of North America, formed part of the western boundary of the Lake Bonneville Basin. This north-south trending range is bounded on the east and west by normal faults, which have elevated and tilted the range to the west (Rodgers, 1989). The range can be broken up into three zones: the southern zone, which is extensively folded late Proterozoic metasedimentary and Precambrian rocks; the Ibapah Stock in the center, dated at ~39 million years ago; and the northern Deep Creek Range, which consists of weakly metamorphosed westward-dipping strata ranging in age from late Proterozoic to Mississippian (Bick, 1966; Thompson, 1973; Rodgers, 1989). The range rises from a desert playa on its eastern flank to the highest point, Ibapah Peak, 3,684 meters. Among many of the east-trending canyons is Reilly Wash, which is incised in late Proterozoic to Lower Ordovician/Upper Cambrian-aged strata

(Rodgers, 1989; Hintze et al., 2000). This incision caused the deposition of a large alluvial fan at its base, which waves and currents in Lake Bonneville cannibalized and redeposited the sediments to the south to form the Reilly Wash Spit Complex.

G.K. Gilbert investigated the Deep Creek Range during his winter field season of 1879, where he traveled from Salt Lake City through the Old River Bed to the Deep Creek Range and Snake Valley (Hunt, 1981). His visit to the spit-bar complex at the base of Reilly Wash Canyon (denoted Willow Springs in his notes and 1890 monograph) lasted three days (Figures 4 and 5) along with the brief mention of a hook spit to the northeast (Figure 6). His field work included taking altitudinal measurements of the spit-bar complex, documenting intermediate embankments, and exploring the internal stratigraphy via incised gullies along the eastern flank of the Deep Creeks. Since Gilbert's visit, this area has not been investigated in as much detail as other prominent Bonneville landforms such as the Old River Bed (Oviatt et al., 2003), Point of Mountain (Schofield, 2004; Gregory, 2006), and Stockton Bar (Burr and Currey, 1992). This study focuses on possible paleoclimate implications preserved in the spit complex's intermediate shorelines and the possibility of undocumented tectonic activity in the Deep Creek Range.

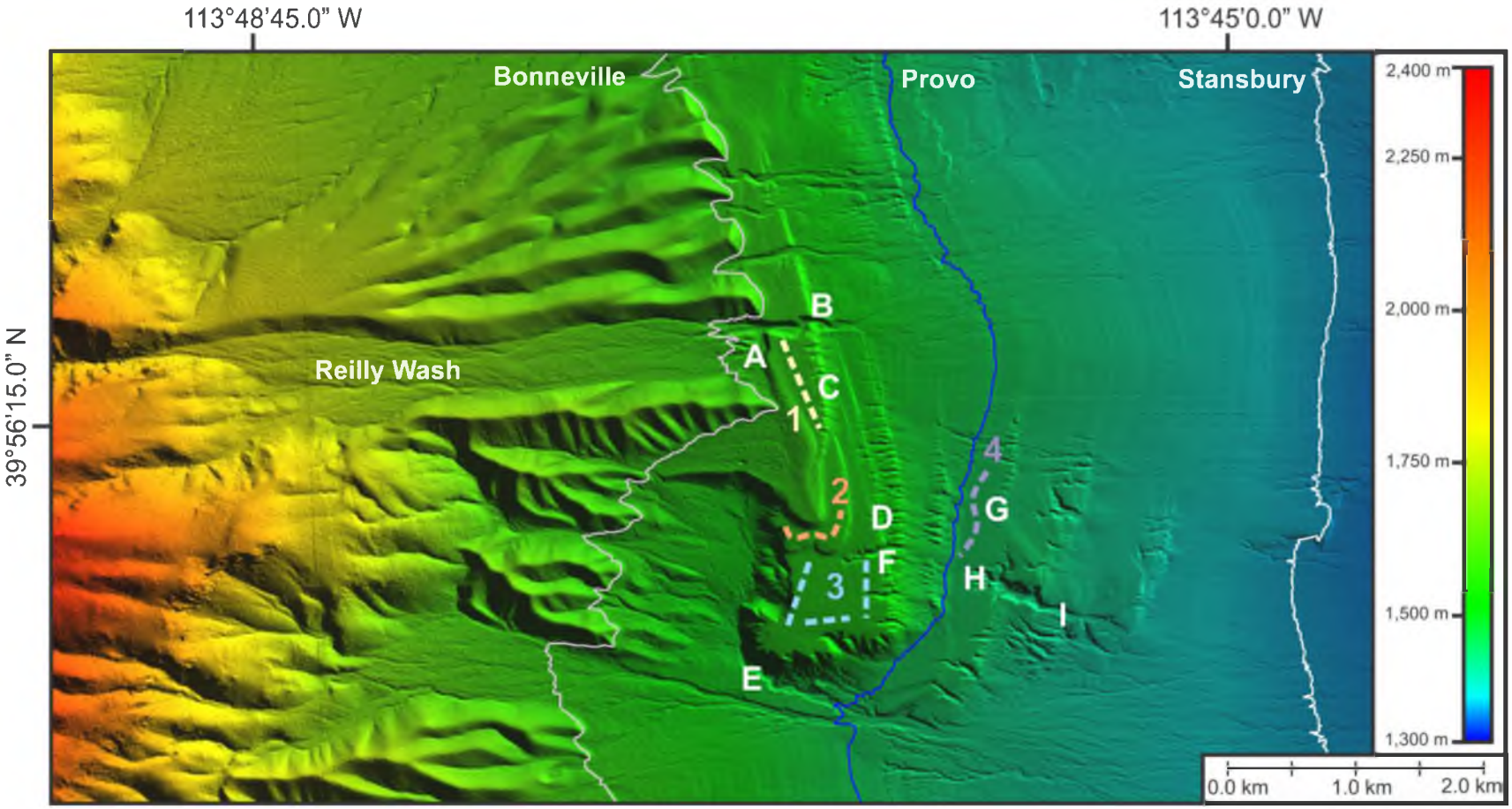

Figure 5. Hill-shaded DEM of Reilly Wash Spit Complex. Numbered dashed lines represent transects for clast size analysis. A) Reilly Wash, B) Reilly Wash boulder line, C) Sampled tufa location, D) Badger Hole, E) Distal boulder line F) Sampled tufa location, G) Scorpion Trench, H) Knife Gully upper, I) Knife Gully lower. For location, refer to Figure 2.

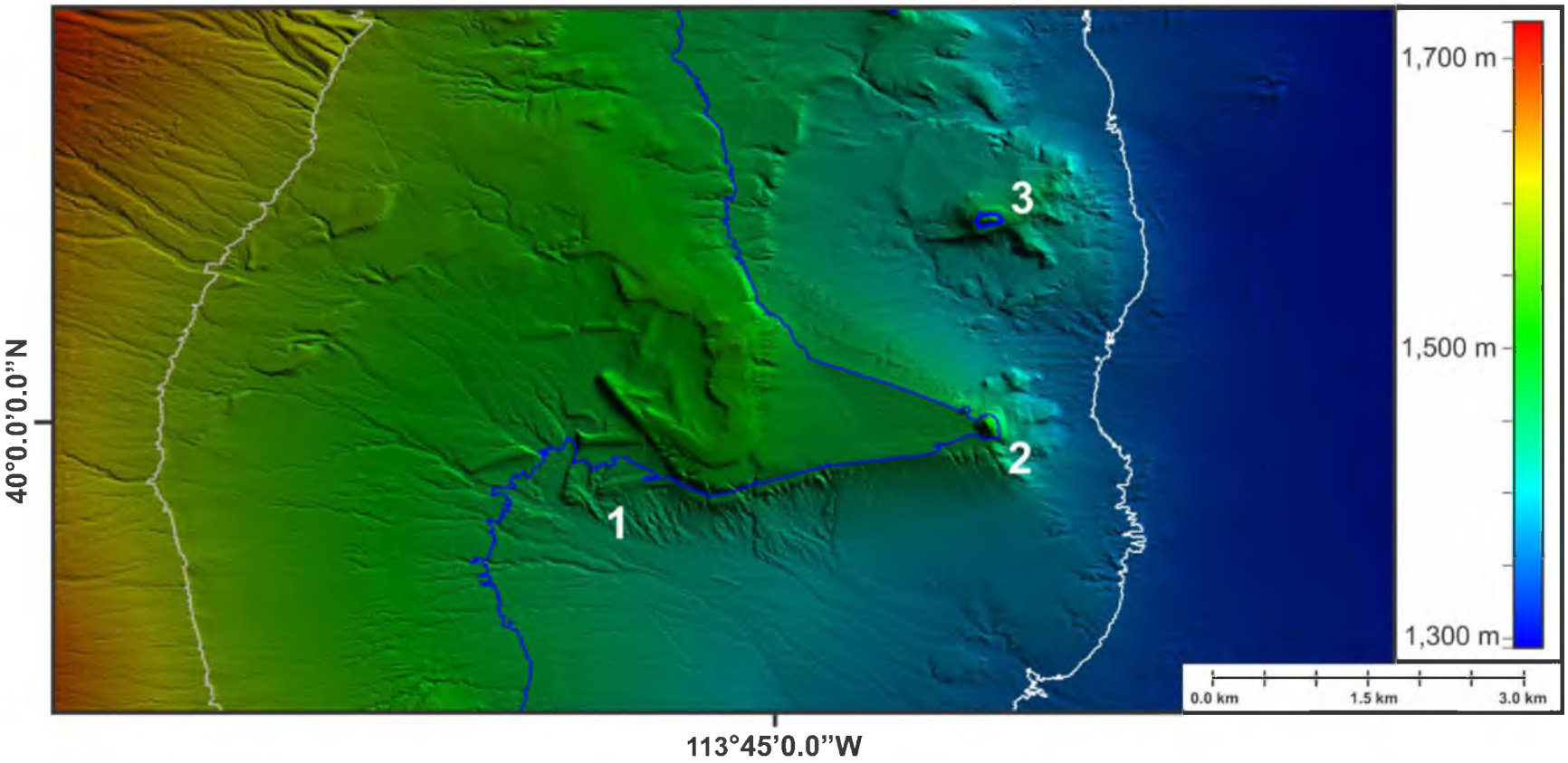

Figure 6. Hill-shaded DEM of a hook spit and tombolo. 1) Tombolo Marl Dump, 2) Inselberg Ephemeral Cut, 3) Tufa Drape (Tufa Analysis). For location, refer to Figure 2.

METHODS

Mapping

Radiocarbon dating and geographic information systems (GIS) software, coupled with high-resolution imagery, provides an opportunity to revisit areas of the Bonneville basin and search for new evidence of the timing and processes of deposition. Constraining the depositional chronology of the lake has been a focus for many researchers (Oviatt, 1997; Godsey et al., 2005, 2011) who have refined Gilbert's original hydrograph (Figure 3). Isostatic adjustment models (Oviatt, 1992) have given geologists the ability to identify the approximate altitudes of the deposition of materials collected for radiometric dating. Isostatic rebound is as much as 60 meters in the central parts of the Bonneville basin.

Aerial photography and digital elevation models allow researchers to observe more of the basin than possible by foot. Initial geomorphic landform analysis was performed in Global Mapper 15 (GM 15) using hill-shades of 5-meter digital elevation models (DEM) and aerial photos obtained from the Utah Automated Geographic Reference Center, along with topographic and geologic maps (Rodgers, 1989; Hintze et al., 2000). Remote mapping has been used to indicate prominent paleo-directions of wind and waves by using the orientation of lacustrine landforms and sedimentary structures, such as spits, barriers, baymouth-bars, and dunes (Gilbert, 1890; Adams and Wesnousky, 1998; Kirst, 2001; Jewell, 2007). Geographic information system (GIS) software was utilized

to calculate tectonic geomorphic indices to define the relative tectonic activity of an area. This is done by observing variations in topography and changes in fluvial systems, which when combined, can help classify relative uplift or inactivity of a mountain front (Bull and McFadden, 1977; Bull, 1984; Zovoili, 2004; Bull, 2007).

By understanding the forces acting upon lake shorelines and sediments, wave development, shear stress from wind and water, and sediment transport can be determined. Past climatic events and predominant regional winds formed the large landforms of Lake Bonneville (Kirst, 2001; Jewell, 2007). Paleolacustrine research on Lake Lahontan, another large Great Basin pluvial lake of the Late Pleistocene, used lacustrine depositional features to infer longshore transport and paleowave heights and velocities (Adams and Wesnousky, 1998; Adams, 2003, 2004). This was accomplished through standard wave theories (Airy; Shields) and their relationships to particle size and threshold velocity to initiate mobilization (Clifton and Dingler, 1984; Adams, 2003). These methods are replicated in this study from clast measurements on Reilly Wash Spit Complex shore platforms in order to estimate paleowave-height and wind direction in the western portion of the Bonneville basin.

Morphometric Indices

Relative tectonic activity of a mountain front can be derived from calculated morphometric indices such as mountain front sinuosity, valley floor width-to-height ratio, asymmetry factor, stream length-gradient index, and basin

hypsometry. These indices are used in this study to help highlight tectonic trends and areas of higher tectonic activity in order to help determine the depositional mechanism of the Reilly Wash alluvial fan and the relative tectonic activity of the range as a whole.

Mountain Front Sinuosity (Smf)

Mountain front sinuosity (Smf) is the ratio of the full length of the mountain piedmont junction (L_{mf}) to the straight-line length of the mountain front (L_s) (Figure 7 A).

$$Smf = \left(\frac{Lmf}{Ls}\right) \quad (1)$$

The mountain-piedmont junction (L_{mf}) is the contact between Tertiary-Quaternary alluvium (TQal) and various lithological units of the range fronts and was determined using Rodgers' (1989) geologic map. In tectonically active ranges, rivers have less time to incise and erode valleys, which leads to a more linear mountain front and a sinuosity closer to 1. Less active mountain fronts have larger embayment's due to greater lateral erosion and sinuosity can be as high as 7 (Bull and McFadden, 1977).

Valley Floor Width-to-Height Ratio (Vf)

Valley floor width-to-height ratio (Figure 7 B) describes the heights of the left (E_{ld}) and right (E_{rd}) divides of a cross valley profile to the width (V_{fw}) facing downstream and altitude of the valley floor (E_{sc}).

$$Vf = \frac{2Vfw}{[(Eld + Esc) + (Erd + Esc)]} \quad (2)$$

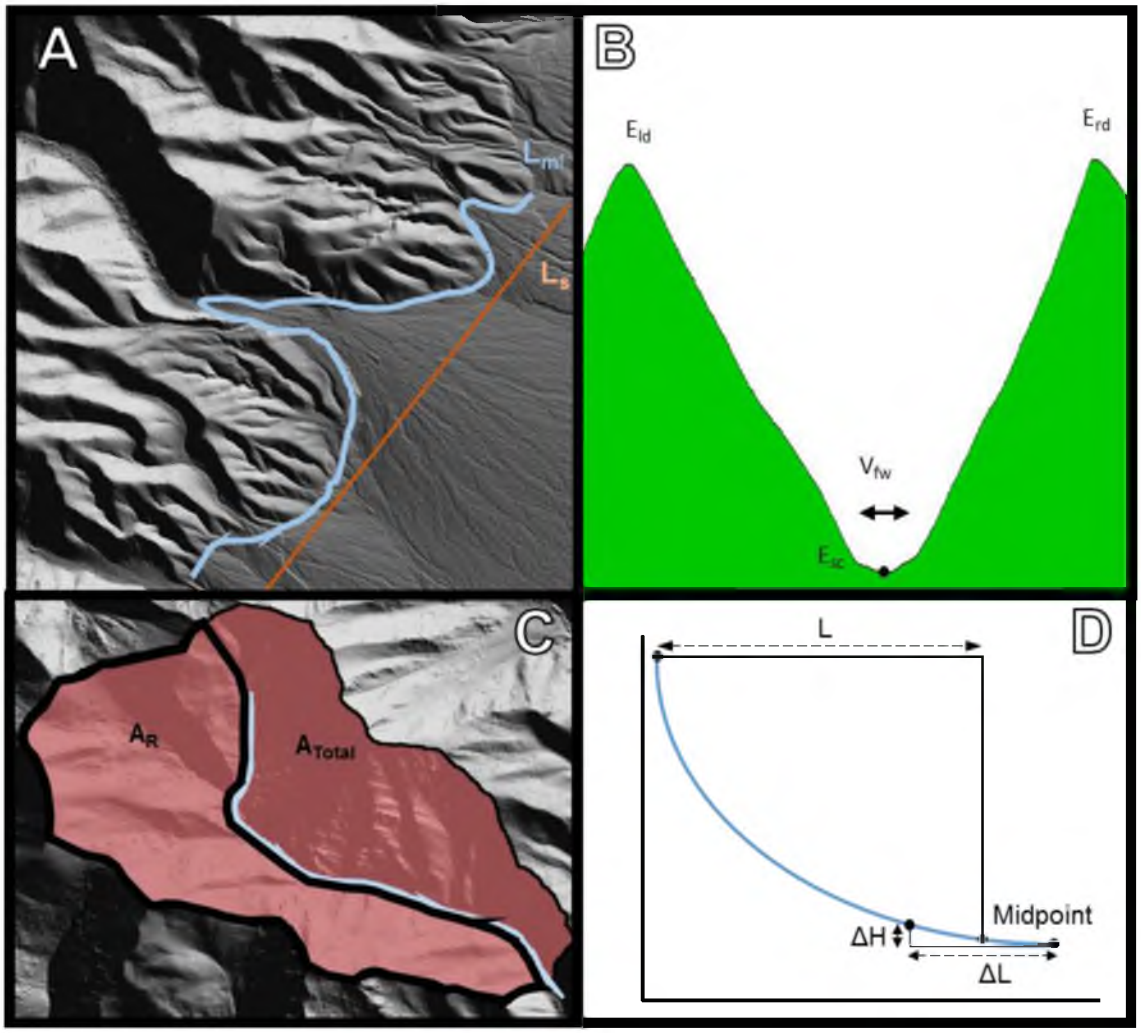

Figure 7. Geomorphic indices and examples of calculation methods: A) Mountain front sinuosity, B) Valley width-to-height ratio, C) Asymmetry factor, and D) Stream length-gradient index.

The width of a valley floor will increase with the termination of uplift, as reflected by an increase in watershed size due to the erosion potential of mountain streams (Bull, 2007). Tectonically active areas will have incised gorges with high relief and narrow valleys (V-shaped), which will result in a low calculated ratio.

To ensure this ratio represents the relative degree of tectonic activity, care must be taken in site selection. V_f was calculated 300-600 m upstream from the mountain-piedmont junction (determined from geologic maps of the Deep Creek Range) to ensure the calculation was made on bedrock and not incised alluvium. It is also important to measure the profile line perpendicular to the stream so the full erosional profile of the river valley can be taken into account, along with taking glaciation into account due to the possible false representation of valley shape in relation to river maturity.

Asymmetry Factor (AF)

Due to variations in lithologic units and lack of previous documentation, a useful index to detect regional uplift is the asymmetry factor (AF). The Asymmetry Factor (AF) index (Figure 7 C) is used to detect possible tectonic tilting of a mountain range (Keller and Pinter, 2002; Pérez-Peña et al., 2010). AF is calculated through the division of the downstream right portion of a watershed split by the main river trunk (Ar) to its whole (At)

$$AF = \left(\frac{Ar}{At}\right) 100 \quad (4)$$

A value of 50 indicates a symmetric basin and any deviation indicates direction of tilt.

Stream Gradient-Length Index (SL)

Stream Gradient-Length index (SL) is used to determine whether a given stream reach has had time to reach equilibrium, which is only achieved in areas of low tectonic activity (Figure 7 D). This index is sensitive to changes in topography and the erosional resistance of the strata. The index can be determined by analyzing the spatial variations of the slope compared to the reach length defined by Hack (1973) as:

$$SL = \left(\frac{\Delta H}{\Delta L}\right) L \quad (3)$$

where ΔH is the change in height between selected contour intervals, ΔL is the length of the river segment between contour intervals, and L is calculated from the midpoint of the river segment (ΔL) to the drainage divide (Zovoili, 2004; Bull, 2007). This index is useful for comparing rivers of various sizes and orders since the gradient (ΔH/ΔL) of a segment is normalized with respect of the length to the drainage divide (L) (Font et al., 2012). 25-meter contours were created from DEMs and used to compute the variables for the SL index and to generate an interpolated map. ArcGIS was used to create an interpolated SL map with classified ranges of SL values.

Basin Hypsometry

The hypsometric curve or hypsometric integral (HI) is used to describe basin hypsometry, which is the area distribution at different elevations within the basin of interest (Strahler, 1952). The hypsometric curve represents the relative proportion of area below or above a given altitude at a given point within a

defined drainage basin. The hypsometric integral relates to the area below the hypsometric curve and therefore is correlated to the shape of the curve, which can be used to highlight the maturity of a given basin (Keller and Pinter, 2002; Pérez-Peña et al., 2010). An immature basin is considered tectonically active due to being in a state of dynamic equilibrium (Hack, 1973). Results are plotted as the relative area, valued 0-1, against each relative height (0-1) (Strahler, 1952). Akin to the SL index, the hypsometric curve can be used to compare catchments of different sizes by comparing the area and elevation between two contours to the total area elevation of the watershed and repeating for each contour interval (Pérez-Peña et al., 2010). The hypsometric curves and the area under the curve (hypsometric integral) were calculated with ArcGIS.

Classifying Geomorphic Indices

The classification scheme of Bull (2007) was used in this study to classify relative tectonic activity. For example, areas of high to moderate activity in the Quaternary will have a V-shaped profile (low V_f), deep fanhead trenches, entrenched alluvial fans, and dark surficial pavements (Pleistocene age alluvial surfaces). Another indicator is watersheds with an "hourglass" shape, which means a narrow neck and a wider upper catchment. These classification schemes were developed from work on mountain ranges in the Basin and Range, and Sierra Nevada, where other pluvial lakes were present during the Late Pleistocene (Bull and McFadden, 1977; Benson et al., 1990).

Volumetrics

Volume calculations of individual shore platforms and landforms were performed with the "Measure Volume Between Surfaces" tool in Global Mapper 15, which also has the ability to measure volumes of "piles" and is used as a first order approximation of the spit complex's volume. Pile boundaries are determined by polygons drawn in GM 15 and the elevations of each of the vertices on a DEM. Thickness of the three-dimensional rasters was based off of average shore slope and vertical distance between shore platforms and used to estimate volumes between selected shorelines.

Field Sampling and Processing

Field investigations of the Reilly Canyon Wash and associated geomorphic landforms include stratigraphic descriptions based on grain characteristics (size, degree of rounding, composition, and orientation), stratigraphic relations, color (Munsell Color, 1991), sedimentary structures, and fossiliferous material such as ostracods and gastropods. All sampled location coordinates were recorded by a handheld GPS (Garmin Etrex 20). Field investigations and subsequent information gained from outcrops are used to constrain a depositional chronology of the spit complex to determine the timing of numerous intermediate shorelines.

Fossiliferous sediments containing freshwater gastropods (genus: *Stagnicola* and *Pyrgulopsis*) were sampled to bracket the depositional chronology of the lacustrine landforms. Samples were cleaned with deionized

water and clipped of their tips to remove sediment that might contaminate the results, and were sent to the Arizona Accelerator Mass Spectrometry (AMS) Laboratory for radiocarbon dating. Ages were calibrated using Calib 7.0 (Stuiver et al., 1998) and plotted against altitudes adjusted for isostatic rebound (Oviatt, 1992).

Ostracods were collected from a stepped trench exposure in Reilly Wash Canyon (Figure 6, location A). Sediment samples were collected in Whirl-pak bags and processed using a modified version of Forester (1988) to separate ostracods from the collected sediments. Boiling deionized water and baking soda assisted in the breakup of sediments, along with mixing sodium hexametaphosphate into the solution to help with deflocculation. After being frozen and thawed, the sediments were washed with deionized water in a no. 80 mesh sieve and all ostracods were separated from the remaining sediments and mounted. Identification was performed using a standard binocular reflecting light microscope.

Tufa samples were collected throughout the study area (Figures 4, location A, C, F, H; Figure 5, location 3). Care was taken while collecting each sample to ensure clean, unweathered surfaces from *in situ* outcrops. Samples were chipped into sections and sent to Arizona Quality Thin Sections, where they were trimmed to size and impregnated with epoxy to keep them intact during grinding (up to 1000 grit). Mounted slides were viewed with a Leica binocular microscope under 2.5x magnification, any identifying characteristics were described, and the specimens were photographed.

Wave Height and Wind Velocity

Paleo-sediment transport and wave energies were analyzed using a series of calculations defined by Adams (2003) to approximate wind velocities during the transgression and Provo stage of Lake Bonneville. Critical variables in this analysis are the median (D_{50}) and maximum (D_{max}) clast sizes. Five sites were selected, with areas ranging from .04-.5 km^2. A modified pebble count technique was used to select clasts for measurements (Wolman, 1954; Bunte and Abt, 2001). With a team of two (recorder and measurer), paths were selected and traversed. Every two paces, the measurer bent at the waist with closed eyes and collected the clast that a pencil inserted into his or her boot laces touched. Each sampled area was marked and traversed from one end to the other while walking at 45˚ angles. Each clast was measured with a digital caliper (a, b, c-axis) or cloth metric tape. Although there was a slight bias toward larger clasts (Wolman, 1954; Bunte and Abt, 2001), this procedure was the most efficient method to implement in the field for determining maximum shear stress imparted by waves on the complex.

Analysis of the fetch of wave trains interacting with the Deep Creek Range during the presence of Lake Bonneville was performed digitally by filling a 30-meter DEM in GM15 with water to a selected elevation. From the location of interest, a vector was drawn until it intersected a land mass and then measured. These vectors were drawn nine times with a three degree offset from the original measurement and averaged to yield an approximate fetch for the selected location (CERC, 1984; Komar, 1998).

RESULTS AND DISCUSSION

Lake Bonneville Features

Initial reconnaissance of the Deep Creek Range via DEMs and brief descriptions from Gilbert (1890) resulted in the selection of a prominent spit-bar complex (3 km^2) located at the base of the Reilly Canyon Wash for detailed study (Figure 6). Notable paleo-shorezones preserved on this landform include the Stansbury, Bonneville, and Provo shorelines along with numerous "intermediate embankments" or intermediate shore platforms at altitudes between the Provo and Bonneville shorelines. Gilbert's 1879 (Gilbert, 1890; Hunt, 1981) sketches of Reilly Wash Spit Complex (Figure 4) depict 4 prominent intermediate shorelines (A, C, D, E) in addition to the Provo (PB) and Bonneville (BB). Another large Bonneville feature located 7.5 km to the northeast is a hook spit with a tombolo feature off its eastern flank (Figure 6). The hook spit is an intermediate depositional feature of Lake Bonneville (Figure 3) that was investigated due to its close proximity to Reilly Wash. Data gathered during initial exploration of the hook spit are presented to detail depositional chronology, but are not a main focus of this study.

Stratigraphic Descriptions of Select Shoreline Exposures

The sedimentology and stratigraphy of seven exposures are described in the Reilly Wash Spit Complex. The Badger Hole site (Figure 5, location D) is an intermediate shoreline with a .5-meter exposure capped with marl that overlays calcium carbonate-coated boulder-to-gravel sized clasts (Figure 8 A). Below are gravels with *in situ,* unbroken gastropods that yield an age of 16,260±110 ^{14}C yr B.P. (Table 1, sample G). Calcium carbonate coated clasts represent an active transgressional shoreface where incoming waves degassed on the rocky shore, depositing the carbonate that cemented the pebbles into beachrock (Felton, 2006). Marls are interpreted to have been deposited during a time when the platform was submerged under relatively deep water (below wave base) about 16 ^{14}C kyr B.P. The occurrence of the Bonneville flood at 14.5 ^{14}C kyr B.P. is indicated by a coarser, lighter colored, marl.

Knife Gully (Figure 5, location H, I) is the second largest incised ephemeral gully along the spit-bar complex. All sediments are at least partially calcareous. The shore platform incised by the stream is capped with tufa (Appendix A). The top part of Knife Gully (Figure 8, B) consists of gravel-to-pebble sized clasts, with a calcium carbonate coating underneath the capping tufa. Gastropods (genus: *stagnicolla* and *pyragulopsis*) were found amongst the clasts and yield an age of 12,027±89 ^{14}C yr B.P. (Table 1, sample H).

Below these clasts is a massive, structureless silt unit with mottles (blotches of different colors) and Gleysols (matrix 5YR 5/2 and Gleysols (hydric soil) 5YR 5/6). This unit overlies very fine sand, with some iron oxide staining,

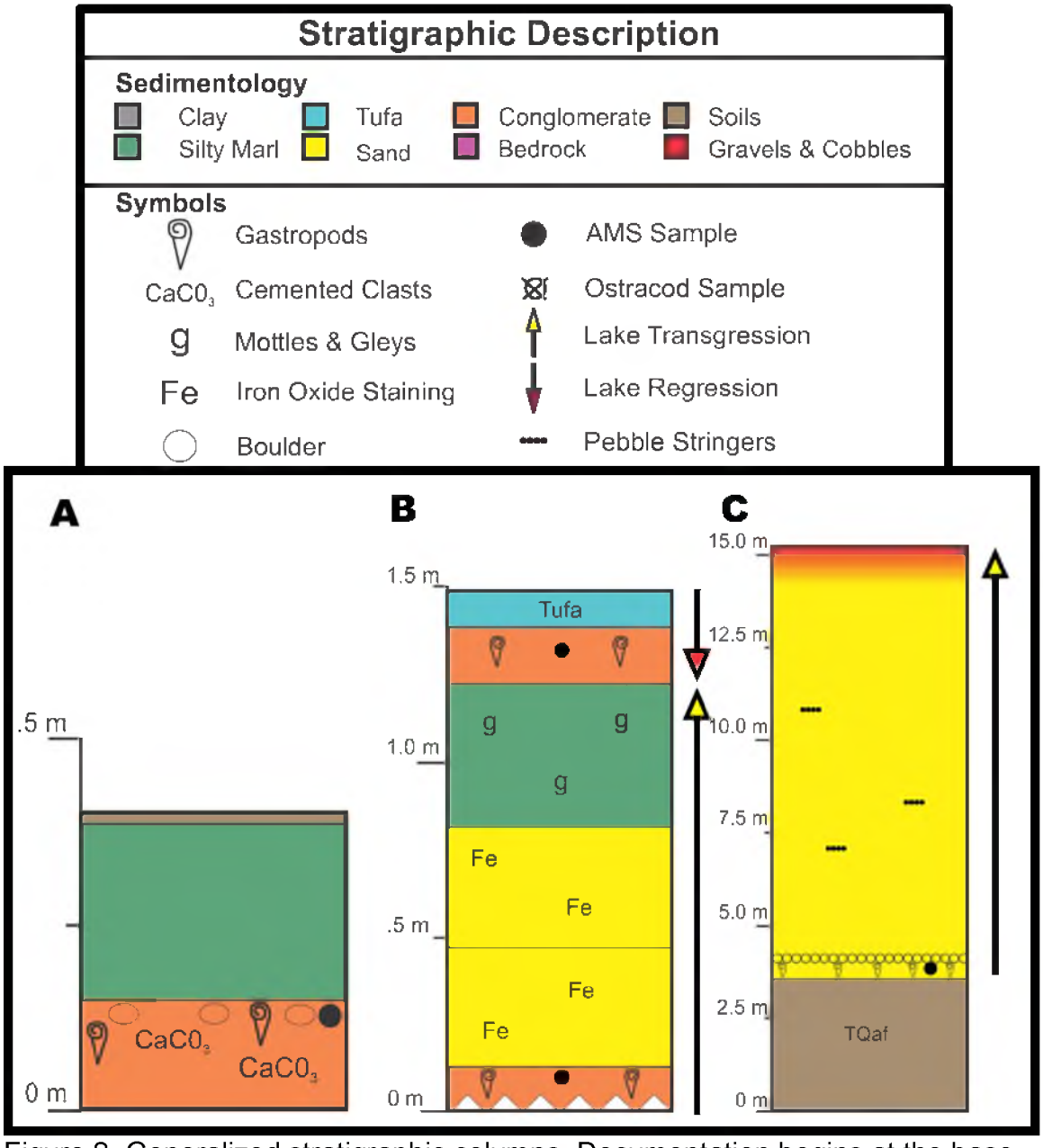

Figure 8. Generalized stratigraphic columns. Documentation begins at the base of the exposure (0 m). Stratigraphic description located at the top of this figure. Locations mapped on Figure 5: A) Badger Hole, B) Upper Knife Gully, C) Distal Exposure

Table 1.AMS C-14 results of dated gastropods.

Locality	Map ID	Material Assessed	Sample Elevation (m a.s.l)	Adjusted Sample Elevation (m a.s.l)[1]	^{14}C age (yr. B.P.)[2]	Cal[3] max	Cal[3] min	δ^{13}C	Lab Code
Badger Hole	G	Gastropod	1535	1508	16260±110	18012	17370	-1	AA102050
Knife Gully Top - Upper	H	Gastropod	1449	1428	12027±89	12178	11757	0.9	AA102051
Knife Gully Top - Lower	C	Gastropod	1449	1428	19920±160	22406	21616	0.1	AA102052
Knife Gully Lower - Upper	I	Gastropod	1423	1404	12334±85	12872	12089	0.2	AA102053
Knife Gully Lower - Basal Gravels	A	Gastropod	1419	1401	20660±140	23345	22501	-0.3	AA102054
Tombolo Marl Dump	B	Gastropod	1430	1411	20230±140	22799	21980	-0.6	AA102055
Isenberg Ephemeral Cut	D	Gastropod	1459	1437	19570±130	21991	21218	0.8	AA102056
Reilly Wash Canyon Boulder Line	F	Gastropod	1559	1528	16670±110	18491	17860	-0.7	AA102057
Distal Boulder Line	E	Gastropod	1496	1471	18060±110	20281	19617	1	AA102058

1. Altitudes adjusted for differential isostatic rebound of basin due to the removal of water (see Oviatt et al., 1992)

2. Dates reported from Accelerated Mass Spectrometer (AMS) with error range.

3. 2-sigma calibrated range using CALIB7.0 (http://radiocarbon.pa.qub.ac.uk/calib/)

and floating pebbles and gravels. Under this is a layer with minimal clay content, iron oxide staining, transitioning to 2-cm scale crumb structures (10YR 6/2 – pale yellowish brown). The base of the exposed unit was cemented gravels and pebbles with *in situ* gastropods, which yielded an age of 19920±160 ^{14}C yr B.P. (Table 1, sample C). Gastropod samples were almost certainly not reworked due to their intact locations among the boulders.

Further down the incised gully is a 5.5 m exposure that displays the internal stratigraphy of the lower portion of the spit-bar complex (Figure 9). A mantle of gravels and cobbles overlies a massive silty marl unit that grades into a sand unit. The sand unit contains a gastropod-rich layer dated at 12,334±85 ^{14}C yr B.P. (Table 1, sample I). The sand unit grades into a marl unit that includes a small number of sand stringers with pebbles throughout. Below is a white marl unit (5YR yellowish grey), that grades into iron oxide stained marl (10YR 7/4 greyish orange). Pebble stringers and hummocky laminations are found throughout the basal portion of the exposure. At the base of this exposure were stage II cemented gravels with occasional cobbles (mostly dolomite). Gastropods above the basal gravel yield an age of 20,660±140 ^{14}C yr B.P. (Table 1, sample A). The transition to lighter colored marl is interrupted by a thin 1-2 cm layer of coarse sand, which has been identified as a Bonneville flood marker (Figure 9, dashed line). This marker is present due to the subsequent reworking of deposited exposed material during the drop in lake elevation and provides an excellent means of correlating strata around the basin (Oviatt, verbal communication, 2013).

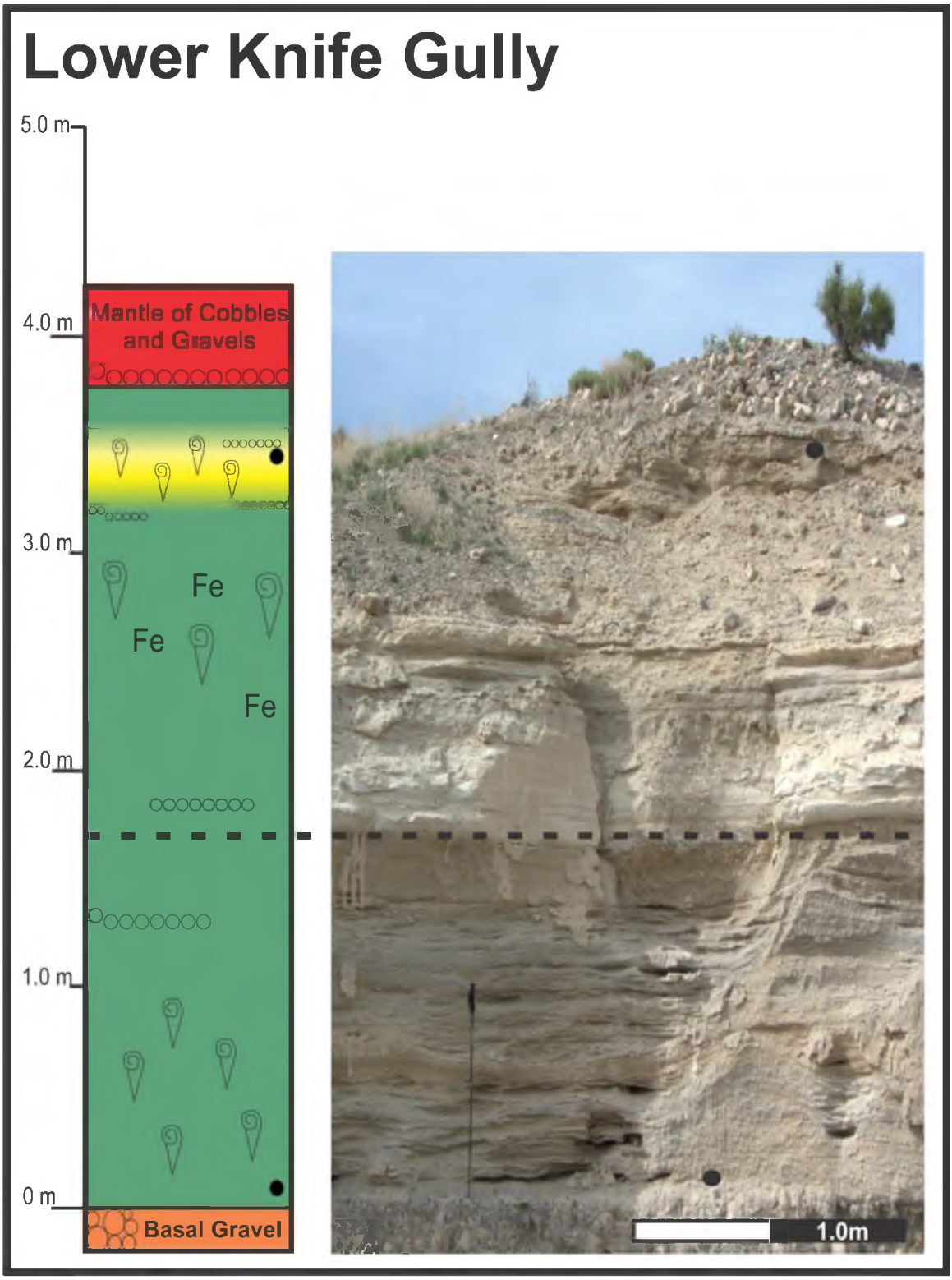

Figure 9. Simplified stratigraphic column of Lower Knife Gully. Black dots represent locations of AMS dated gastropods. Dashed line represents location of Bonneville flood marker. For location, see Figure 5, legend in Figure 8.

Both the upper and lower Knife Gully exposures are interpreted to represent the transgressional phase of Lake Bonneville, the Bonneville flood, and the subsequent Provo phase. Exact timing of transgression between Knife Gully Lower – Basal Gravels (20,660±140 ^{14}C yr B.P.) to Knife Gully Top – Lower (19,920±160 ^{14}C yr B.P.) cannot be determined because the range of error in the calendar ages of the samples overlaps.

A trench was dug at the base Reilly Wash (Figure 5, location A; Figure 10) to sample the sediments for ostracods and record the stratigraphy. Above the trench, the sediments were characterized as heavily varnished desert pavement with weathered quartzite and dolomite clasts. Below the gravel lag was a 3-centimeter thick AV horizon with blocky structures and root traces, superimposed on a layer of stage 0-I cemented gravels grading downward into a very fine sand matrix (10YR 5/4 moderate yellowish brown), and a pebble layer.

Location #1 of Figure 10 denotes a transition into silty marl that superimposes a 12-cm thick gravel lens overlying another silty marl lens with fine laminations. Location #2 signifies an increase in overall clay content, a section with iron oxide stained Gleysols (10 YR 5/4 moderate yellowish brown). Location #3 marks a transition into fine laminations and increasing clay content. Location #4 marks a transition into high clay content, with some clay laminae having a white calcium carbonate coating and a color change in the matrix (10YR 5/2). The base of the trench was cemented gravels with layers of pebbles, sand and gravels, and intermittent cobble-size clasts. Thin section analysis was inconclusive for determining the source of clast cementation (Appendix A).

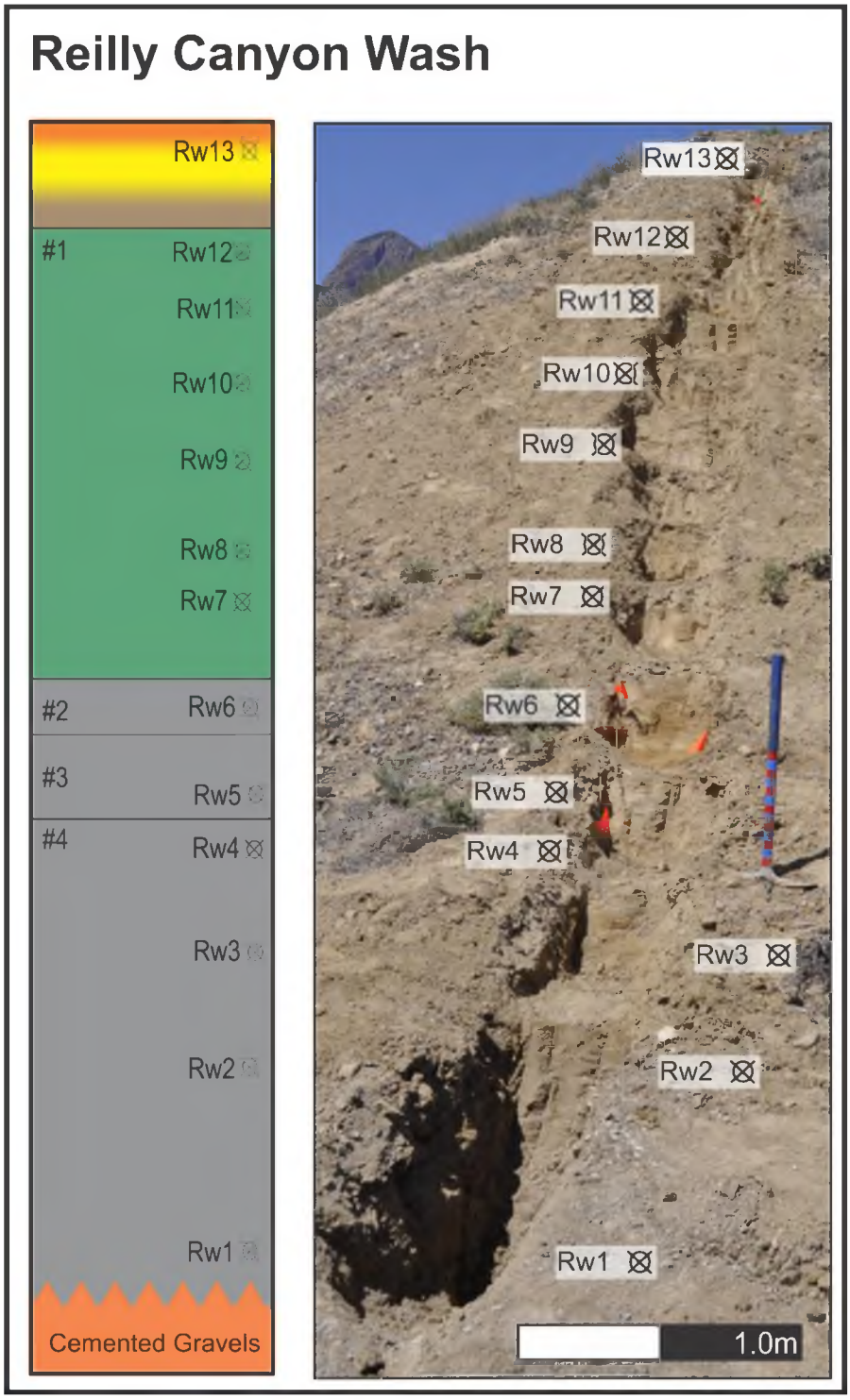

Figure 10. Stepped trench at the base of Reilly Wash (Figure 5, location A). Sediment samples taken for ostracod identification denoted with "Rw#". Numbers 1-4 refer to flags in photo. See legend in Figure 8.

Sediment samples taken for ostracod analysis were inconclusive (Figure 10). Few ostracods were found in these samples. Fragments of juvenile *Candona* sp. were identified in samples RW1 and RW2, along with a few *Candona* sp. and *Limnocythere* sp. in sample RW 12. Identified ostracod fragments were poorly preserved and possibly reworked (Oviatt, digital communication 2014).

The Distal Exposure (Figure 5, location E; Figure 8 C) is capped with gravels that grade downward into a fine to medium fine sand with pebbles throughout. This exposure is on top of a layer of very fine sand with some silts, along with 1-3 centimeter medium sand beds throughout and draped over long aspect ratio boulders with *in situ* gastropods in a medium sand matrix. Below the boulders are paleosols (10YR 5/4 moderate yellowish brown) and stage III calcite soil development. Gastropods yielded an age of 18,060±110 ^{14}C yr B.P. (Table 1, sample E). The sediment below the *in situ* gastropods and boulders is not from lacustrine deposition, based on the stage of soil development, but is believed to be from the pre-Bonneville alluvial fan surface of Reilly Wash. The age dates obtained from gastropods (Table 1, sample E) represent the approximate age of the initial deposition of the main lobe of the RWSC.

Scorpion Trench (Figure 5, location G) is a 0.5-meter thick exposure located on one of the many intermediate shore platforms making up the complex. This exposure lies on the Provo shore platform. Colluvial sediments are overlain by pale yellowish brown (10YR 6/2) silts and clays (minimal clay and stage I $CaCO_3$) that are subsequently overlain by 15 centimeters of stage I-II $CaCO_3$ - cemented gravel clasts (dolomite and quartzite). A structureless massive

(centimeter scale columnar peds), composed of very fine-grained calcium carbonate-rich sands and 2% clays (greyish orange pink, 5YR 7/2) are on top of the gravels and underneath a surface gravel lag. Capping marls are interpreted to represent the transgressional phase of the lake, while cemented clasts and sands are assumed to represent post-flood, Provo lake elevation.

The hook spit with an attached tombolo, northeast of Reilly Wash Spit Complex (Figure 6), contained two areas with material suitable for dating. At the base of the tombolo feature, *in situ* gastropods were found among a basal gravel horizon superimposed by white marl (Figure 6, location 1) that yielded an age of 20,230±140 ^{14}C yr B.P. (Table 1, sample B). On the point of the tombolo is an incised gully (Figure 6, location 2) with gastropods that dated to 19,570±130 ^{14}C yr B.P. (Table 1, sample D). These dates suggest that it took approximately 750-1200 ^{14}C yr for the tombolo to form. The hook spit is interpreted to have been deposited during the transgression of the lake due to its topographically higher elevation than the tombolo.

Tufa samples from Appendix A, are interpreted to be capping tufa, most likely formed in high-energy waters with little sediment supply. Sample from Appendix A, was part of a 4-to-6 meter tall tufa drape, 10-40 centimeters thick, deposited on exposed bedrock (Devonian dolomite, Figure 2) of the tombolo. These tufa deposits were likely formed by degassing of carbonate-rich waters by high-energy waves generated along the large northwest-trending fetch (Fenton, 2006; Oviatt, verbal communication 2013). Tufa samples (Appendix A) are cemented beachrock, found on the shore platform slope and platform/slope

break, respectively. Tufa sample shown in Appendix A, is a beach rock collected from the base of the stepped trench towards the bottom of Reilly Canyon Wash and represents possible lacustrine – fluvial interaction due to the nature of calcium carbonate cement.

Clast Counts and Size Distributions

Clast counts for the four selected shore platforms (Figure 5) resulted in D_{50} calculations ranging from 11.7 to 18.69 cm and D_{MAX} ranging from 24.5 to 47.1 cm (Figures 11, 12). The only noticeable difference among counts is between the upper shore platforms and the Provo bench, for which both D_{50} and D_{MAX} were smaller. This could have been caused from the exposure of the hook spit to wave energy during, and after, the Bonneville flood (Figure 6). This exposure would have disrupted longshore drift, creating a region of reduced wave energy along the shorelines of Reilly Wash Spit Complex. A large tufa drape at approximately the same elevation, and slightly to the northeast of the hook spit (Figure 6, location 3), is the result of this dissipation of wave energy on the exposed bedrock.

Geochronology

AMS C-14 results for the nine collected gastropod samples are shown in the modified Nelson's (2012) hydrograph (Figure 13), which represents a collection of dated material as summarized by Oviatt (1997) and Godsey et al. (2011). Reported dates A-E (Figure 13; Table 1) plot close to the base hydrograph and represent post-Stansbury transgression. Lake Bonneville waters

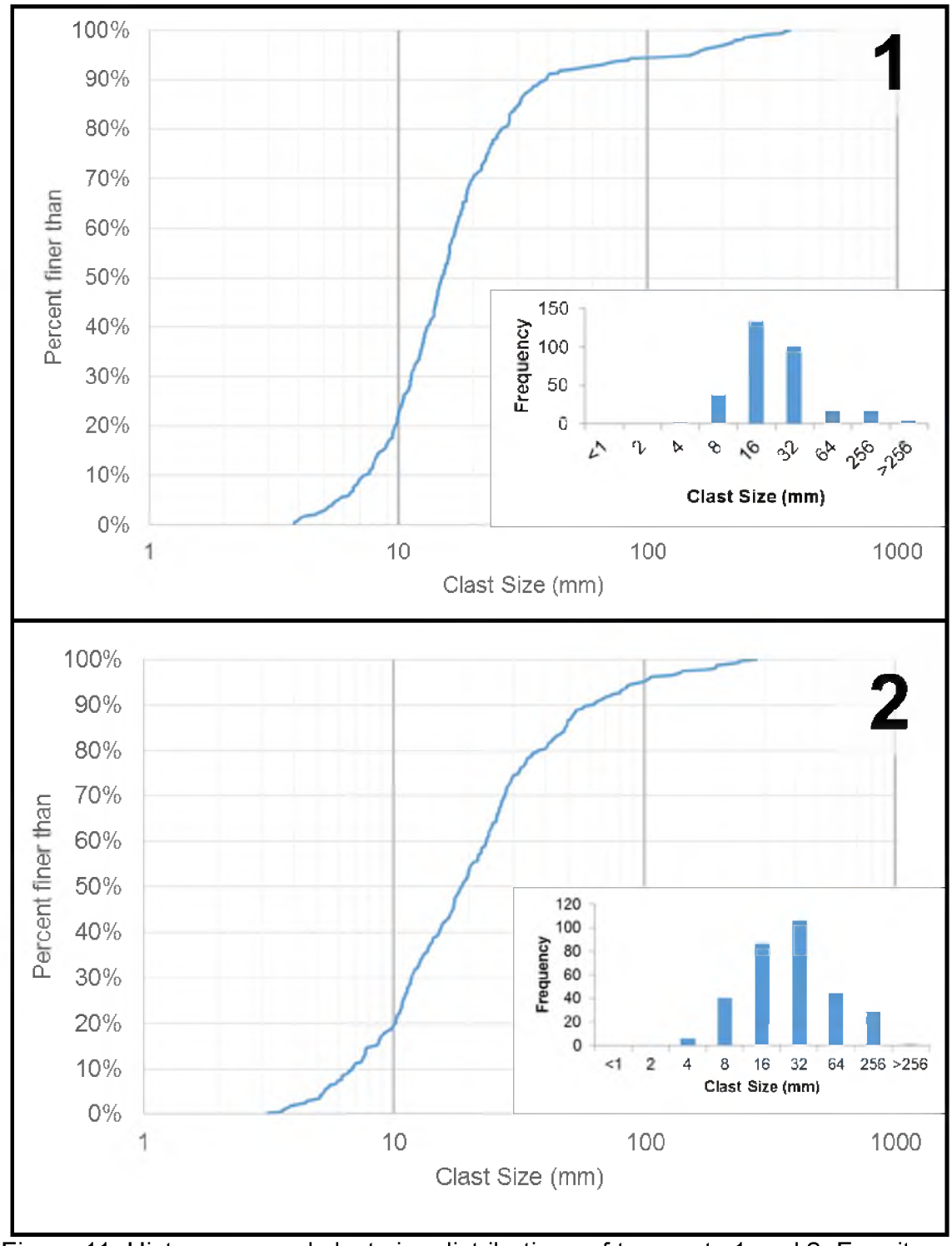

Figure 11. Histograms and clast size distributions of transects 1 and 2. For site locations, refer to Figure 5.

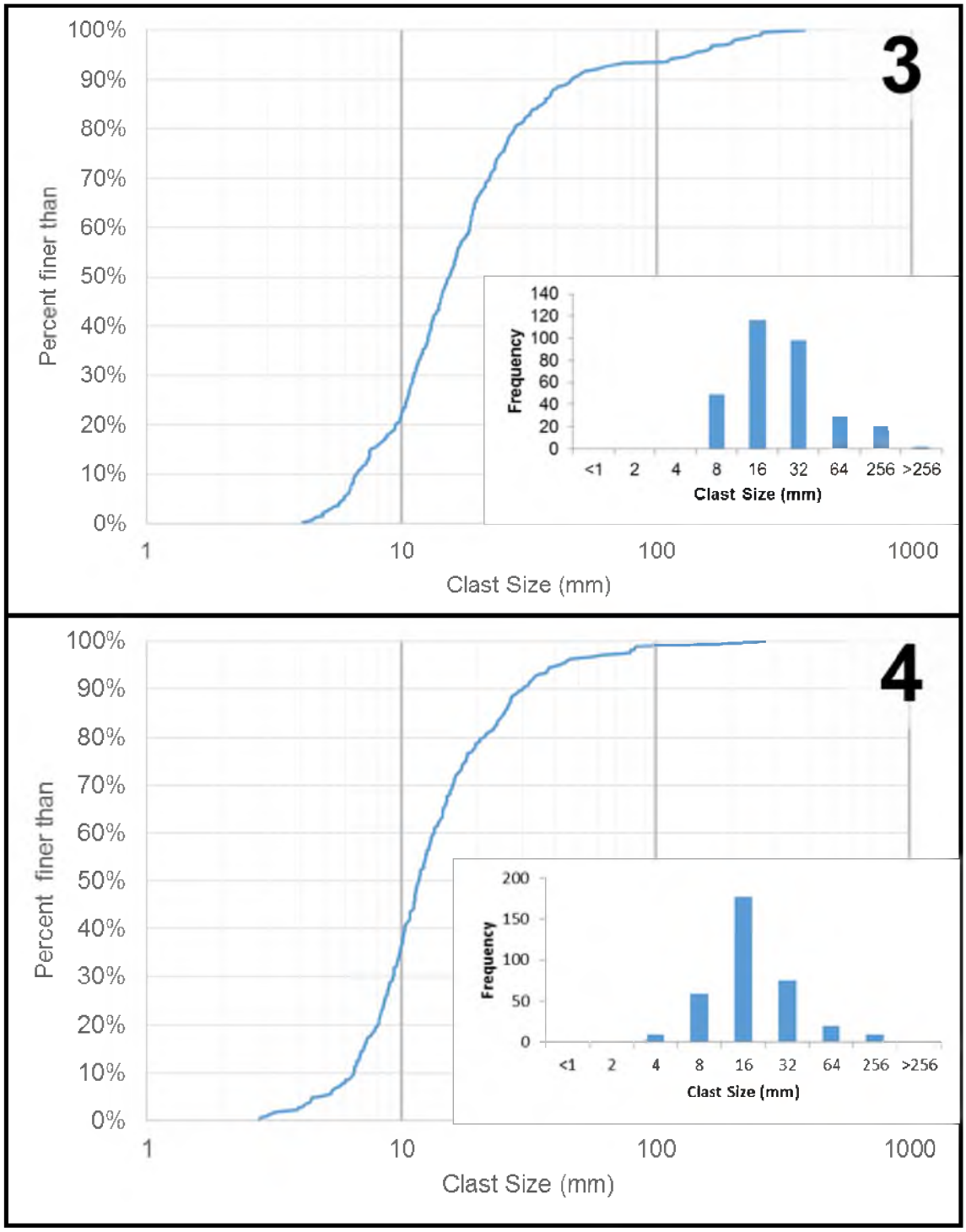

Figure 12. Histograms and clast size distributions of transects 3 and 4. For site locations, refer to Figure 5.

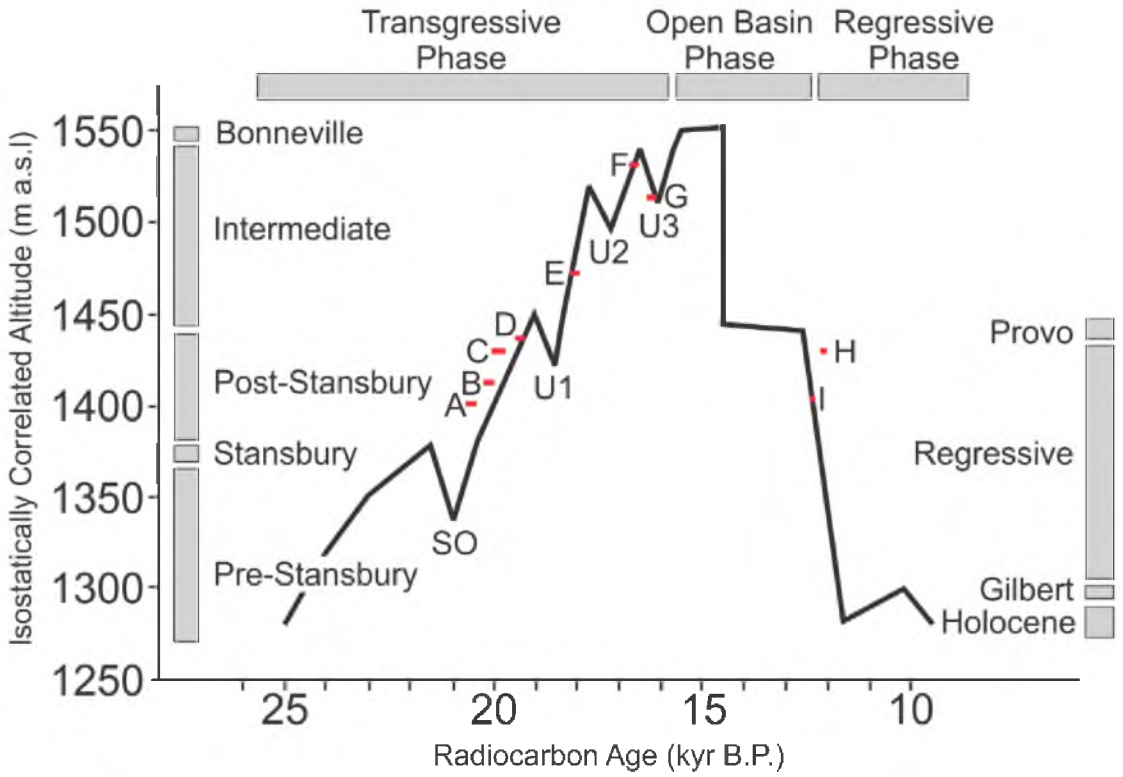

Figure 13. Hydrograph with AMS dated gastropods. Error associated with each date is represented in the length of each of the lines corresponding with a dated gastropod. Letters refer to Table 1. Vertical boxes correlate to different stages of Lake Bonneville. Horizontal boxes represent the three phases of Lake Bonneville (Gilbert, 1890). SO – Stansbury Oscillation, U1 – Unnamed oscillation 1, U2 – Unnamed oscillation 2, U3 – Unnamed oscillation 3 (Oviatt, 1997). Elevations were corrected for isostatic rebound (Oviatt, 1992). Figure modified from Nelson (2012).

might have begun interacting with Deep Creek Range sediments as early as 21 kyr ^{14}C B.P. The tombolo feature northeast of the main spit complex was deposited over approximately 750-1200 ^{14}C yrs (Figure 6, location 1, 2; Table 1, sample B, D; Figure 13, B, D).

Gastropods collected from Badger Hole (Figure 5, location D; Table 1, sample A; Figure 13, A) are the only dated samples from an intermediate shoreline on Reilly Wash Spit Complex. Reilly Wash Boulder Line gastropods (Figure 5, location B; Table 1, F; Figure 13, F) yield an older date than Badger Hole gastropods and were found at a higher elevation. This can be explained by an oscillatory event during the overall transgression of Lake Bonneville.

These two dates bracket the approximate transgressional maximum of oscillation "U2" and maximum regression of oscillation "U3" (Oviatt, 1997; Benson, 2011; Nelson, 2012). Although these reported dates do not match the hydrograph perfectly, algorithms to correct for isostatic rebound are simplified for the whole basin and might not accurately reflect the rebound experienced in the Deep Creeks after the regression of Lake Bonneville. In addition, possible errors from lab analysis (minimal), possibility of postdepositional transport, and contamination of younger carbon through leeching of meteoric waters may explain the variance.

The presence of marls in the Reilly Wash trenched site (Figure 10) indicates a low energy environment (Hunt, 1981). The conditions needed for marl deposition are interpreted to be the result of the barring of the alluvial fan valley. This area would of have been filled with mountain fluvial waters and storm wash-

over. The incision through the spit complex at the base of Reilly Wash can then be implied to have occurred sometime after the Bonneville flood (Hunt, 1981).

Geomorphic Interpretation

Investigations in the Deep Creek Range led to the delineation of 42 watersheds for the calculation of tectonic geomorphic indices (Figure 14). ArcHydro, an ArcGIS extension, was used to calculate flow accumulation and direction, although not all watersheds had perennial streams. Around the range, 11 fronts were calculated for mountain front sinuosity (Figure 14). The highest calculated S_{mf} average value was in the western portion of the range (2.02), while the lowest average was in the north (1.36). The eastern and southern flanks of the range had approximately the same average values, 1.73 and 1.79, respectively (Table 2). Valley floor width-to-height ratios (V_f) were calculated for each watershed. The highest valley floor width-to-height ratio value came from watershed 24, which yielded a value of 0.41 while the lowest was watershed 5 at 0.052 (Table 3).

To better represent the asymmetry of a watershed, and to avoid confusion among the different sections of the mountain front, the absolute value of AF was taken and subtracted from 50 (Pèrez Peña et al., 2010). This approach generates a direction and degree of asymmetry (Figure 14).

$$AF = \left|50 - \left(\frac{AR\ x\ 100}{AT}\right)\right| \quad (5)$$

The most symmetric basin has an AF value of 15 while the most asymmetric basin had an AF value of 31 (Table 3). When mapped, the values were binned

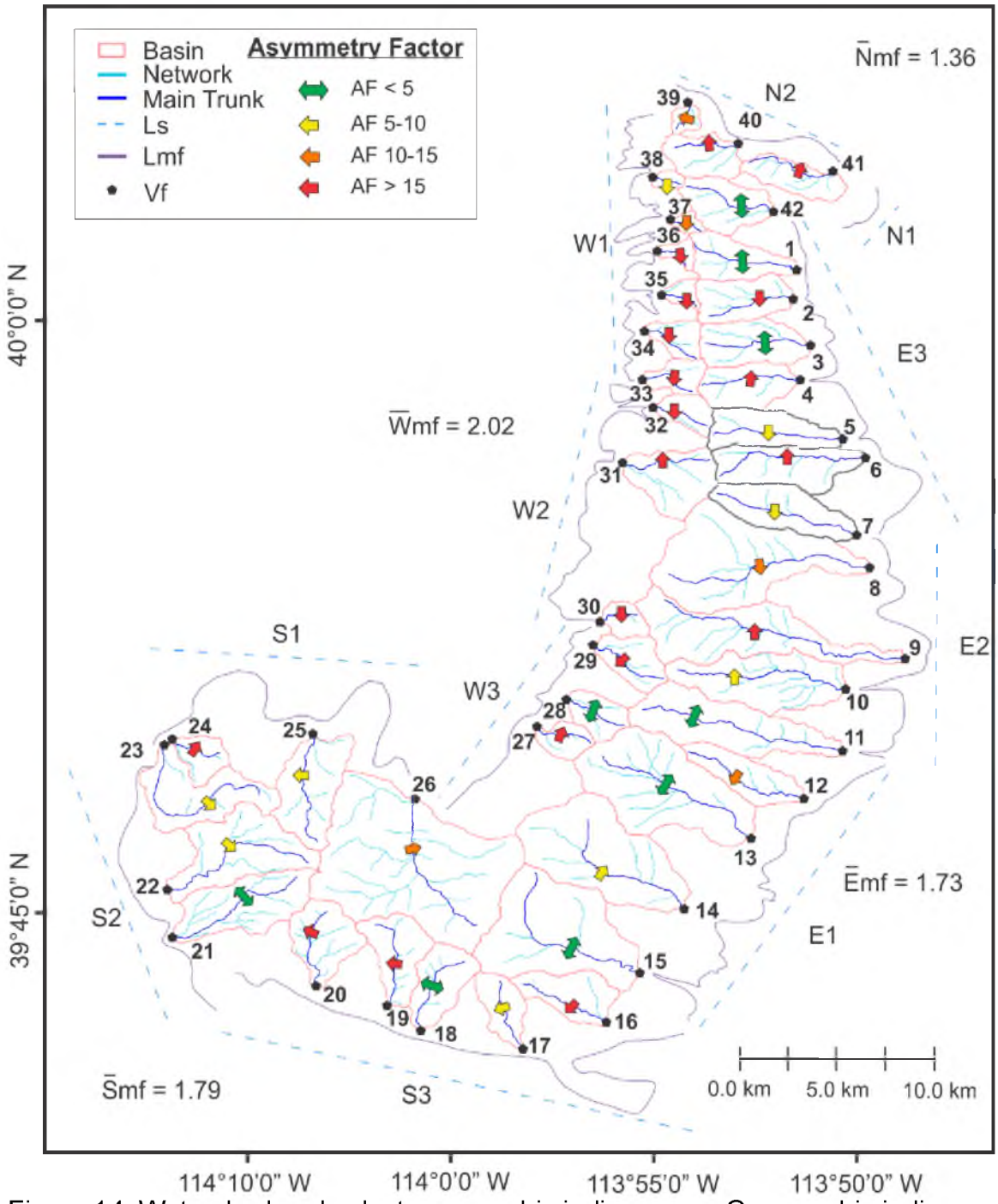

Figure 14. Watershed and select geomorphic indices map. Geomorphic indices include asymmetry factor, mountain front sinuosity, stream network and each watershed's main trunk (modeled after Peña et al., 2010). Watersheds 5-7 are highlighted in grey to denote main area of study. Watershed 6 is Reilly Canyon Wash.

Table 2. Mountain front sinuosity (Smf) results. For site locations, refer to Figure 14. Lmf – Length of mountain front; Ls – Length of the piedmont – mountain junction.

Name	Smf	Lmf	Ls
W1	2.75	35.01	12.74
W2	1.96	22.24	11.35
W3	1.34	12.36	9.24
S1	2.43	23.96	9.86
S2	1.20	15.41	12.86
S3	1.73	30.58	17.66
E1	1.87	26.08	13.94
E2	1.84	19.47	10.61
E3	1.47	22.41	15.20
N1	1.37	3.04	2.22
N2	1.36	9.30	6.84

Table 3. Asymmetry factor (AF) and valley floor width-to-height ratio (Vf) results. Calculated for each designated watershed in the Deep Creeks. Vfw – Valley floor width; Eld – elevation of the left divide; Erd – elevation of right divide; Esc – elevation of stream channel; Vf – Valley floor width-to-height ratio; - AF Asymmetry factor.

Basin	Vfw (m)	Eld (m)	Erd (m)	Esc (m)	Vf	AF
1	15	2052	2084	1919	0.10	1.44
2	26	2135	2157	1936	0.12	18.09
3	35	2019	2126	1897	0.20	2.10
4	44	2270	2144	2037	0.26	15.15
5	14	2332	2364	2078	0.05	8.91
6	18	2088	2119	1942	0.11	16.76
7	19	2142	2186	1951	0.09	8.41
8	16	1926	1956	1807	0.12	14.61
9	26	1786	1695	1608	0.19	15.73
10	59	2288	2076	1801	0.16	8.65
11	40	2016	1947	1781	0.20	1.13
12	28	2025	1982	1812	0.15	14.66
13	60	2348	2260	1917	0.16	4.03
14	41	2282	2281	2021	0.16	6.53
15	72	2413	2556	1697	0.09	0.75
16	30	2575	2023	1951	0.09	25.90
17	12	2096	2099	2059	0.32	5.12
18	28	2457	2366	2239	0.16	2.71
19	37	2368	2351	2208	0.24	15.09
20	18	2253	2246	2160	0.20	18.96
21	16	2119	2163	2077	0.24	2.22
22	27	2360	2287	2151	0.16	10.00
23	20	2096	2116	2035	0.29	6.69
24	11	2118	2114	2062	0.20	14.66
25	33	2182	2142	2080	0.41	7.55
26	30	2240	2214	2129	0.30	13.97
27	12	2510	2440	2342	0.09	17.20
28	17	2762	2646	2467	0.07	1.67
29	16	2486	2543	2377	0.11	15.26
30	14	2610	2509	2335	0.06	19.35
31	18	2303	2288	2118	0.10	29.77
32	11	2241	2219	2137	0.12	15.67
33	11	2152	2131	2043	0.11	19.02
34	15	2104	2077	1999	0.17	27.66
35	11	2155	2104	2061	0.17	25.86
36	5	1994	2022	1981	0.19	20.93
37	16	2159	2110	2036	0.16	10.90
38	21	2095	2047	1969	0.21	7.93
39	10	1945	1919	1880	0.20	10.48
40	12	1962	2013	1938	0.24	26.66
41	32	1846	1919	1770	0.28	31.83
42	25	2075	2013	1966	0.32	3.95

into classes similar to Pèrez Peña et al. (2010), with arrows representing each of the classes: AF < 5 (symmetric), AF= 5-10, AF= 10-15, and AF > 15 (asymmetric).

Results of hypsometric curves for each basin were combined based on the segment of the S_{mf} they fall along. Hypsometric curves plotted for each basin (Appendix B) and the hypsometric integral (area under the hypsometric curve) were classified based on the standard deviation of values and mapped (Figure 15).

A stream length-gradient (SL) index was calculated at each 25-meter contour interval along the main trunk of each watershed. Using ArcGIS's inverse distance weighting interpolation tool, a map was created to show areas of higher (anomalous) SL index values (Figure 16). Geometrical Interval classification scheme was used to bin the data into 10 categories, which is helpful when dealing with data that are not distributed normally and assists when visualizing data (IDW Interpolation Map of SL Index values, Figure 16).

The most useful indices for interpreting higher tectonic activity in this study were the hypsometric curve and hypsometric integral, due to their ability to highlight less mature watersheds, which corresponds to higher relative tectonic activity (Bull, 2007). Normal faulting in the northern portion of the Deep Creek Range might have been present during the late Tertiary and Quaternary (Rodgers, 1989). Watersheds in the northern portion of the range, specifically those not affected by glaciation north of the Ibapah Stock have high hypsometric

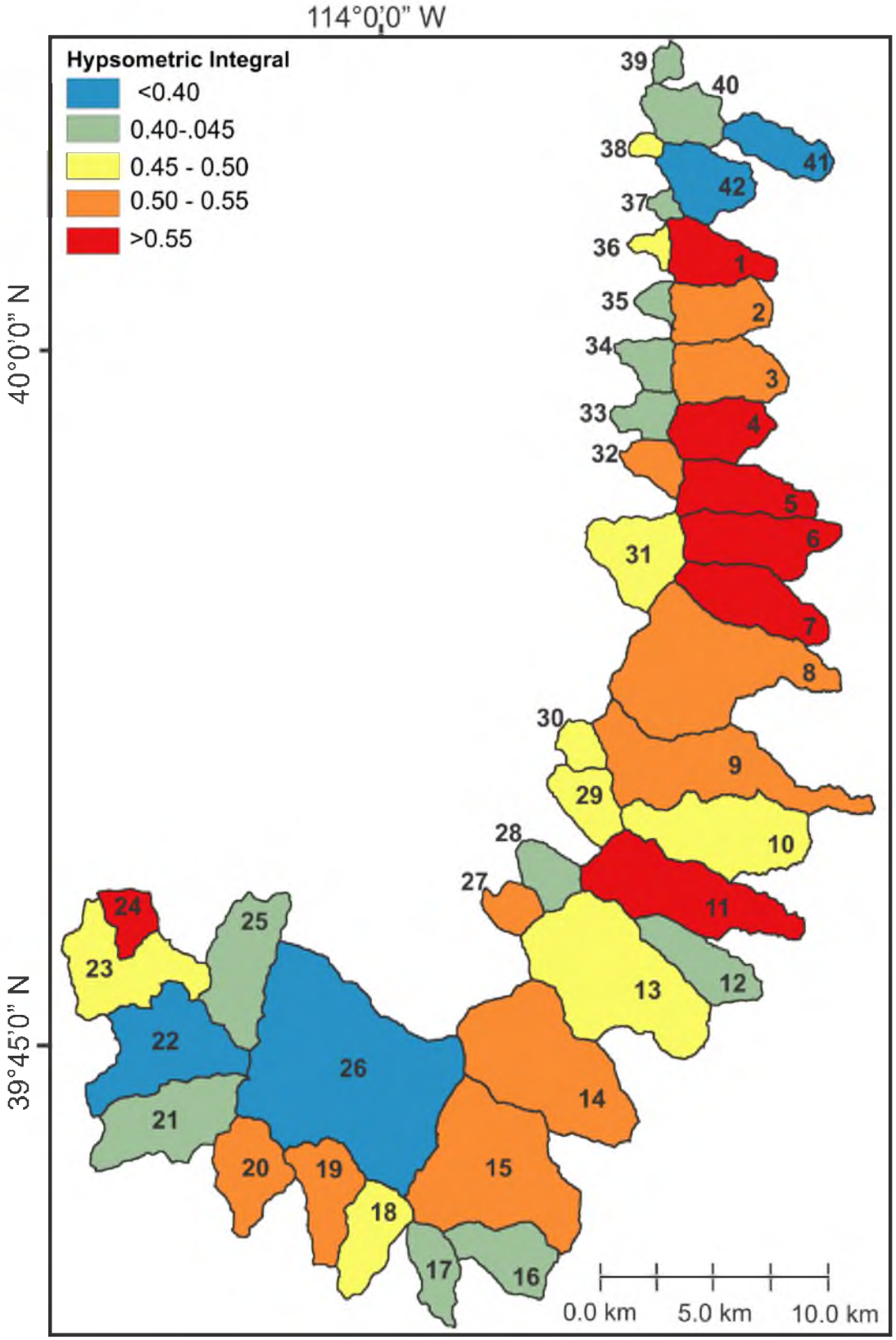

Figure 15. Map of hypsometric integral results. Spit complex is located at the base of watershed 6.

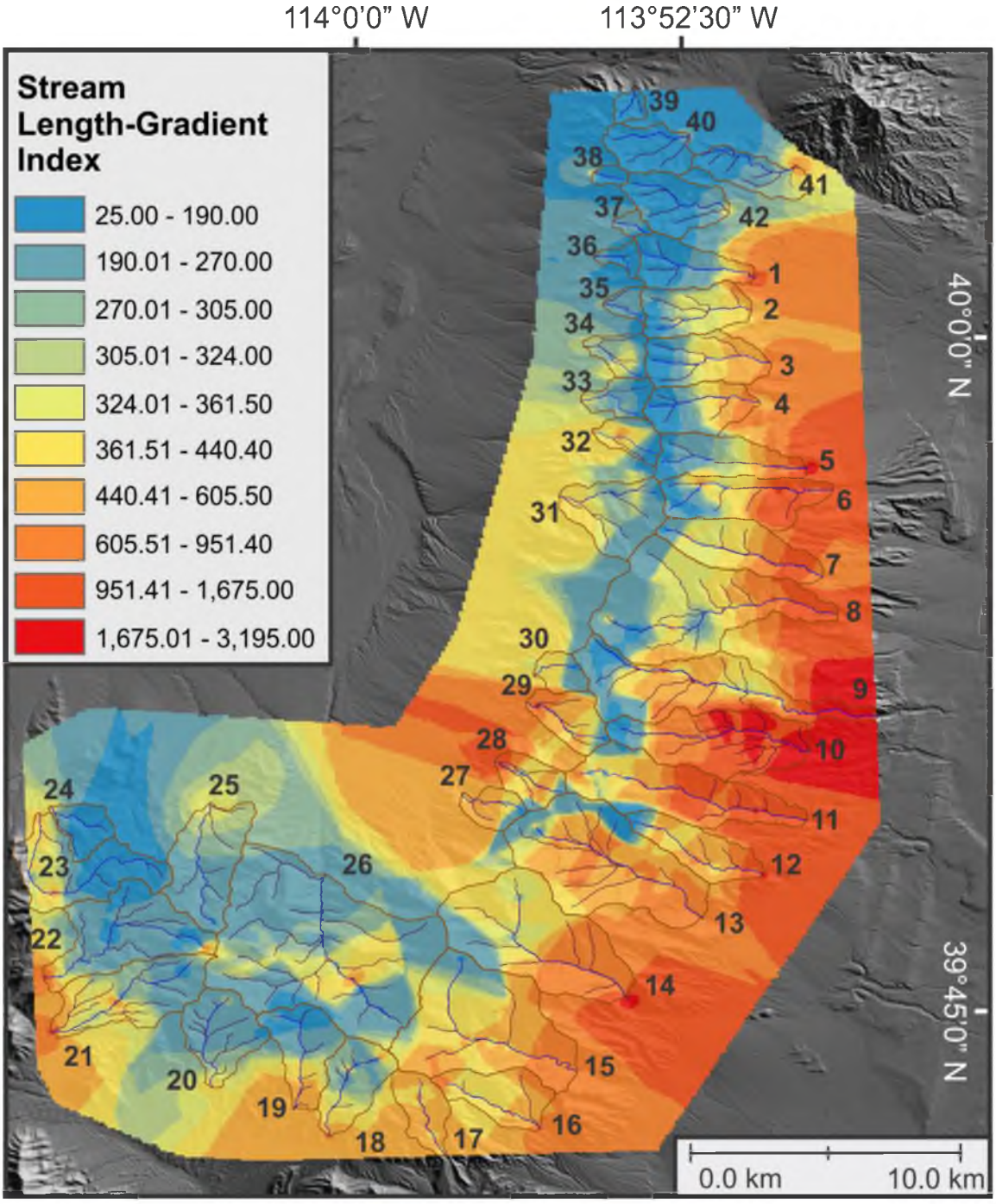

Figure 16. Inverse Distance Weighting (IDW) interpolation map of calculated SL index values. Higher values indicate anomalies along the longitudinal profile. Spit complex is located at the base of watershed 6.

integrals, which represents general erosional immaturity (Strahler, 1952; Keller and Pinter, 2002; Pèrez Peña et al., 2009). Reilly Canyon has one of the highest HI of all of the watersheds, which might correspond to tectonic activity causing the disruption of the watershed's evolution. Based on the hypsometric data, the alluvial fan deposited at the base of Reilly Canyon (watershed 6) is most likely a result of tectonic activity during the late Tertiary and Quaternary (exposing weakly metamorphosed late Proterozoic to Mississippian strata) and not the result of large mass-wasting events.

Other geomorphic indices used in this project to determine relative tectonic activity were not as useful as the hypsometric integral. The stream length-gradient index is not a good indicator when there are several transitions from easily erodible units (weakly metamorphosed units in the northern Deep Creeks) to those more resistant to erosion, such as the quartzite at the head of Reilly Canyon's alluvial fan (Bull, 2007). Also, during the Holocene, this range has received less precipitation than during the Late Pleistocene and thus makes it problematic to trust the results of ephemeral streams, which represent half of the studied watersheds (Keller and Pinter, 2002; Bull, 2007).

The asymmetry factor (AF), which is used to assist in identifying possible fold propagation and tectonic tilting, was inconclusive in the Deep Creek Range. The only area that shows any pattern is the northwestern watersheds (Figure 14 and Table 3, 31-38) possibly due to activity along the western north-south trending normal fault or the Rocky Springs Thrust (Rodgers, 1989).

The southeastern portion of the range (Figure 14 and Table 3, 8-15) was

glaciated, which affects the reliability of using geomorphic indices for investigating relative tectonic activity. Two indices supporting recent activity in the northeastern portion of the basin are mountain front sinuosity (S_{mf}) and valley floor width-to-height ratio (V_f). S_{mf} values for the segment that includes Reilly Canyon Wash (Figure 15, W3) are in the lowest three of the eleven calculated segments. V_f values for Reilly Wash and the watershed to the north are low compared to the rest of the range and are classified as being relatively seismically active (Silva et al., 2003; Bull, 2007).

The alluvial fans deposited at the base of Reilly Canyon Wash and the watershed to the south are the only two distinctive fans in the Deep Creek range and both have been incised with evidence of meandering stream paths. These incisions were made prior to the transgression of Lake Bonneville and subsequent wave action has reworked and deposited the eroded sediments into the Reilly Wash Spit Complex.

Based on the results of three calculated indices, S_{mf}, V_f, HI, the hourglass shape of the watershed, and the presence of deep fan head trenches and dark surficial pavements, both the deposition and incision of the alluvial fans are determined to have been the result of previously undocumented tectonic activity in the Quaternary near watersheds 4-7 (Figure 15,16).

Sediment Volumes and Flux Rate

The large size of the spit complex compared to others in the basin (Figure 17) is interpreted to be due to the constant supply of sediment from Reilly Wash

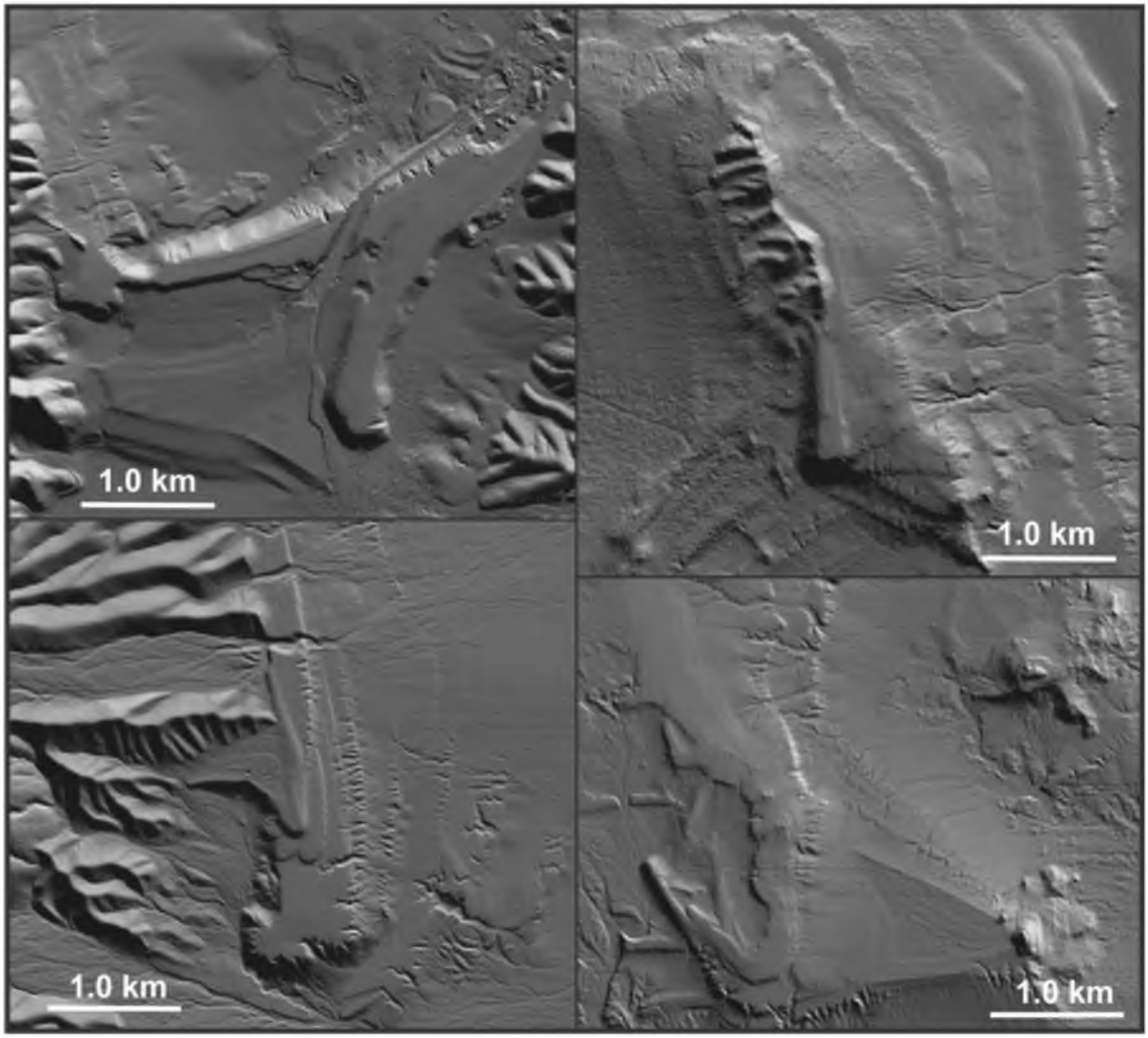

Figure 17. Comparison of spit and bar landforms in the Lake Bonneville basin. A) Stockton Bar, B) Hogup spit, C) Reilly Wash Spit Complex, D) hook spit.

(relative immaturity) and the preexisting alluvial fan. The main lobe of the spit complex, extending from the large incised gully of Reilly Wash, yields an estimated volume of 75 million cubic meters. Volumes were broken down based on prominent intermediate shorelines (Figure 18). This resulted in the selection of five sediment packages angled at 3°, the average slope of the five shorelines and the angle used in paleowind-speed and wave height calculations. Sediment flux rates were calculated using ages of dated gastropods from Knife Gully Top Lower (19,920±160 ^{14}C yr), Badger Hole (16,260±110 ^{14}C yr) and approximate timing of the Bonneville flood (14,500 ^{14}C yr).

The range of time between the lowest dated gastropod of the spit complex and the Bonneville flood is ~5,400 ^{14}C B.P., which yields a 1.3 x 10^4 m^3/yr sediment flux rate. This can be broken down into smaller increments by calculating the sedimentation rate from Knife Gully Top Lower to Badger Hole (1.2 x 10^4 m^3/yr) and Badger Hole to the Bonneville flood (1.5 x 10^4 m^3/yr).

Due to a lack of research on Lake Bonneville spit sediment flux rates, it is hard to compare this spit to others throughout the basin. Comparing rates to modern analogs is not quite the same due to differing variables (e.g., marine vs. lacustrine, fetch, and wind regimes). Johnson (1956) states that sediment flux rates for the southwestern portion of modern Lake Michigan are between 0.6-7 x 10^4 m^3/yr. Based on the amount of sediment and the size of the spit complex, it is thought that transport occurred during storm events due to the discrepancies between D_{MAX} and D_{50} of the measured clasts on all of the shorelines (Johnson, 1956).

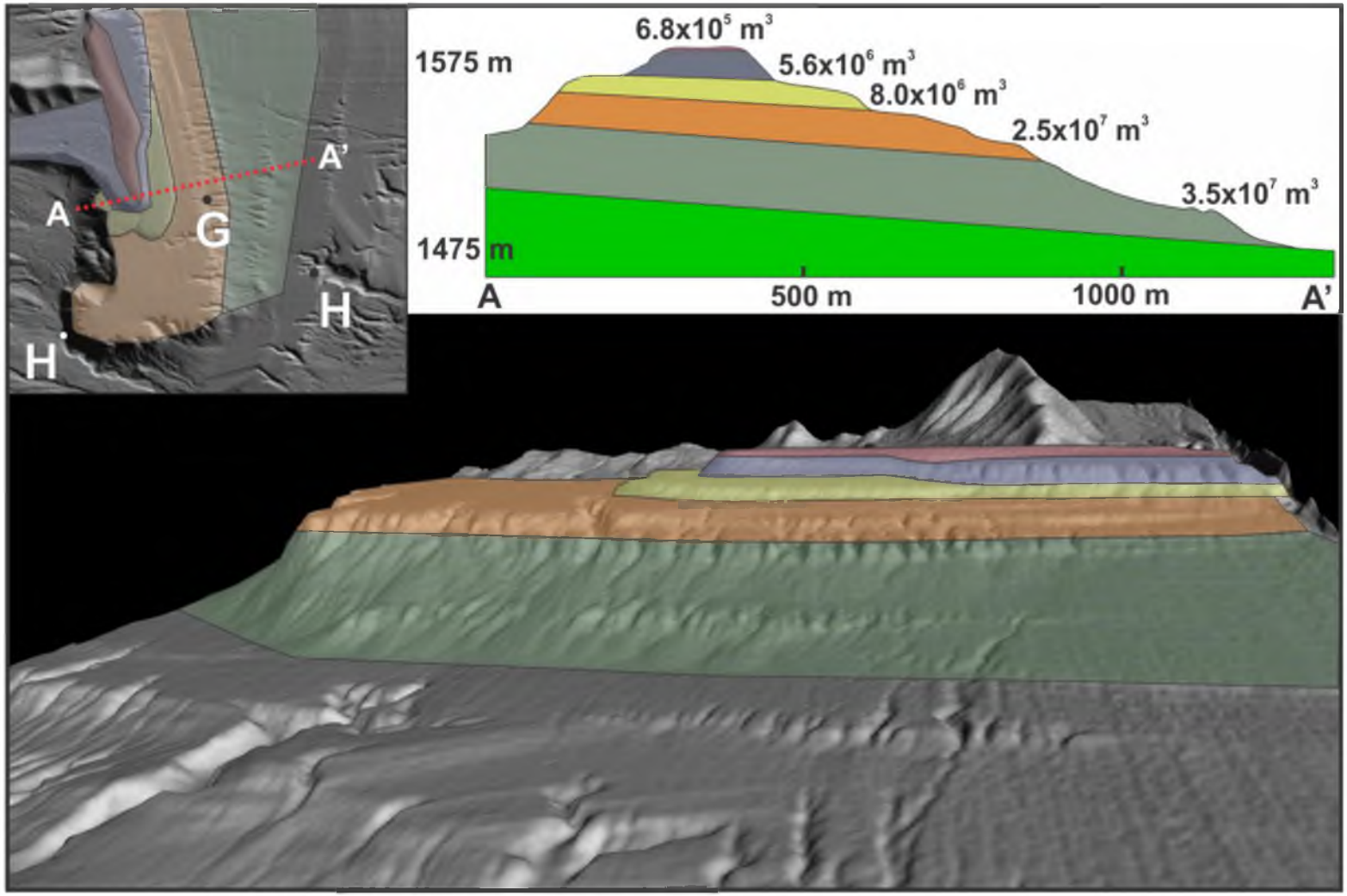

Figure 18. Spit complex volume calculations. Top Left: Map view of the spit complex and profile cross-section. Top right: Profile view of volume calculations with calculated volumes. Letters in plan-view (not A-A`) refer to dated gastropod samples (Table 1).

Paleowind Estimation and Interpretations

Four sites on the spit complex were chosen for clast size analysis, one at the Provo elevation, two on intermediate shorelines, and one near the Bonneville maximum (Figure 5, locations 1-4). Figures 11 and 12 show histograms and size distributions of b-axis measurements from the four selected sites. D_{MAX} and D_{50} for each transect have been used for paleowind and wave height calculations, similar to Adams' (2003) beach particle technique (BPT) to estimate wind velocity and deep water wave height required to transport measured clasts. This technique was based on modern strong wind events and transported clasts on a Great Salt Lake gravel beach. Although Adams (2003) uses some assumptions in his calculations (e.g., period, fetch-limited, and wave steepness), his method is used in this study as an estimate of possible wind speeds derived from clast measurements, which were deposited during the transgression and regression of Late Pleistocene Lake Bonneville. The assumption of fetch-limited conditions is based on the Shore Protection Manual and nomograms of observed wind speed, wave height, storm duration, fetch length, and wave period (CERC, 1984).

An average fetch of 100 km was calculated in a north-northeast (NNE) to east-northeast (ENE) trend. This direction was chosen because of the north to south orientation of the spit complex (Figure 19), which can be used as a proxy for direction of blowing winds (Evans, 1942; Jewell, 2007). The calculated fetch results in periods of 5.5-8 seconds (CERC, 1983; Adams, 2003; Manly, 2012). These variables were used to calculate an estimated paleowave-height and wind speed (at 10 meters) using equations 1-12 of Adams (2003). Calculated wind

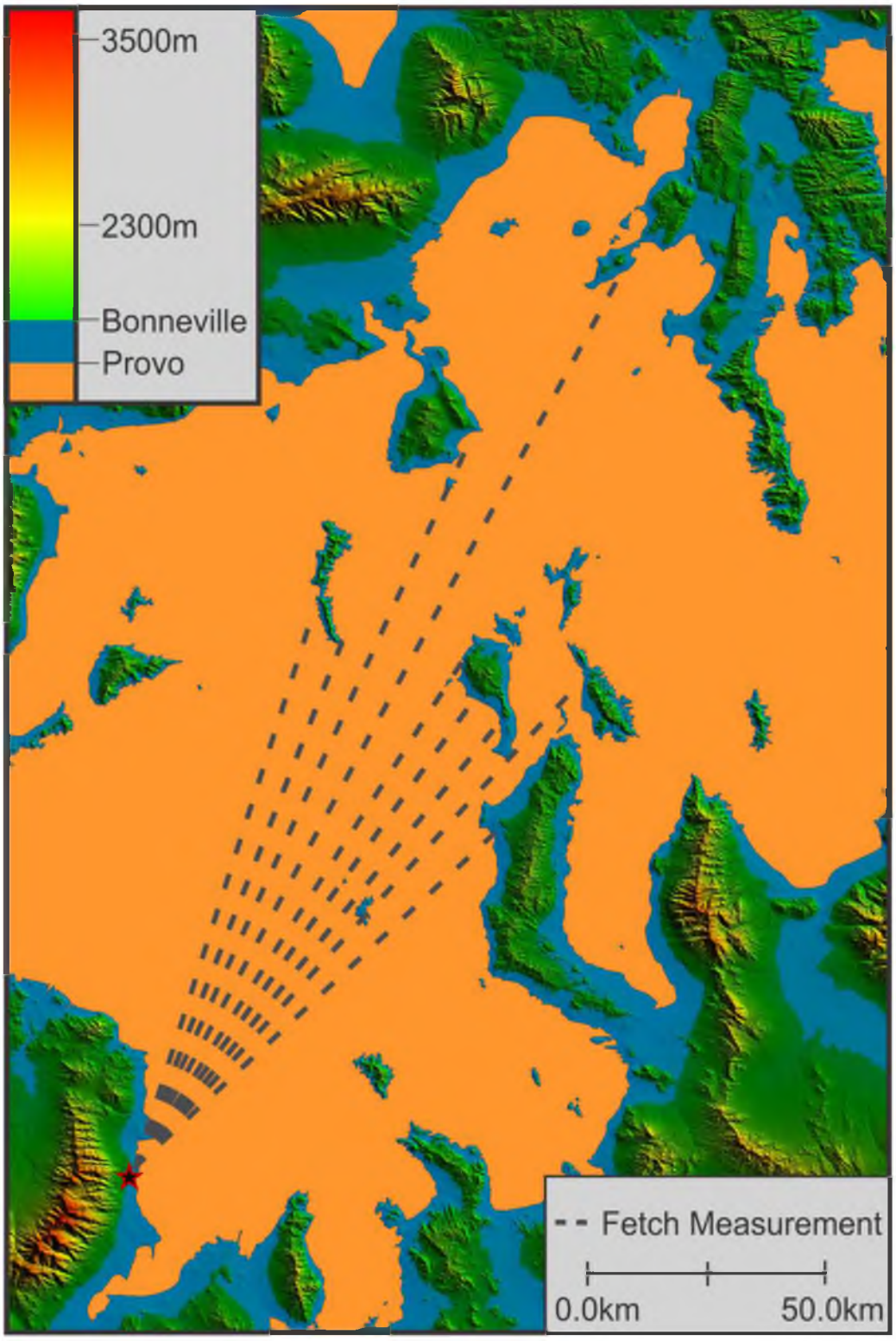

Figure 19. Map of estimated maximum fetch from Reilly Wash Spit Complex. Star symbolizes spit complex location.

velocities ranged from 13.1 – 18.4 m/s and wave heights varied between 2.7 and 4.1 m (Table 4).

To compare estimated wind velocities from the Late Pleistocene to the present, wind records were compiled from MesoWest for Callao, UT (April 2000-February 2014) (Figure 1). Wind rose plots were created to visualize wind data, including binned direction percentage (blowing from indicated azimuth) and mean vector (Figures 19). Compared to present-day wind speeds compiled from the nearby town of Callao, UT (Figure 20), which are mainly southerlies, estimated Late Pleistocene winds are slightly higher in magnitude and predominately from the north, as confirmed through the orientation of the spit complex (Orme and Orme, 1991; Jewell, 2007).

Table 4. Estimated paleowave height and wind velocity results. For site locations, refer to Figure 5.

Site	Fetch (km, azimuth)	Beach Slope (degrees)	D_{MAX} (b-axis, cm)	D_{50} (b-axis, cm)	Estimated deep-water wave height (m)	Estimated wind speed ($m\ s^{-1}$)
1	100 NW	3	29.11	15.33	4.03	18.03
2	100 NW	3	47.14	18.59	2.95	14.00
3	100 NW	3	33.09	14.88	4.03	18.03
4	100 NW	3	24.48	11.72	2.72	13.12

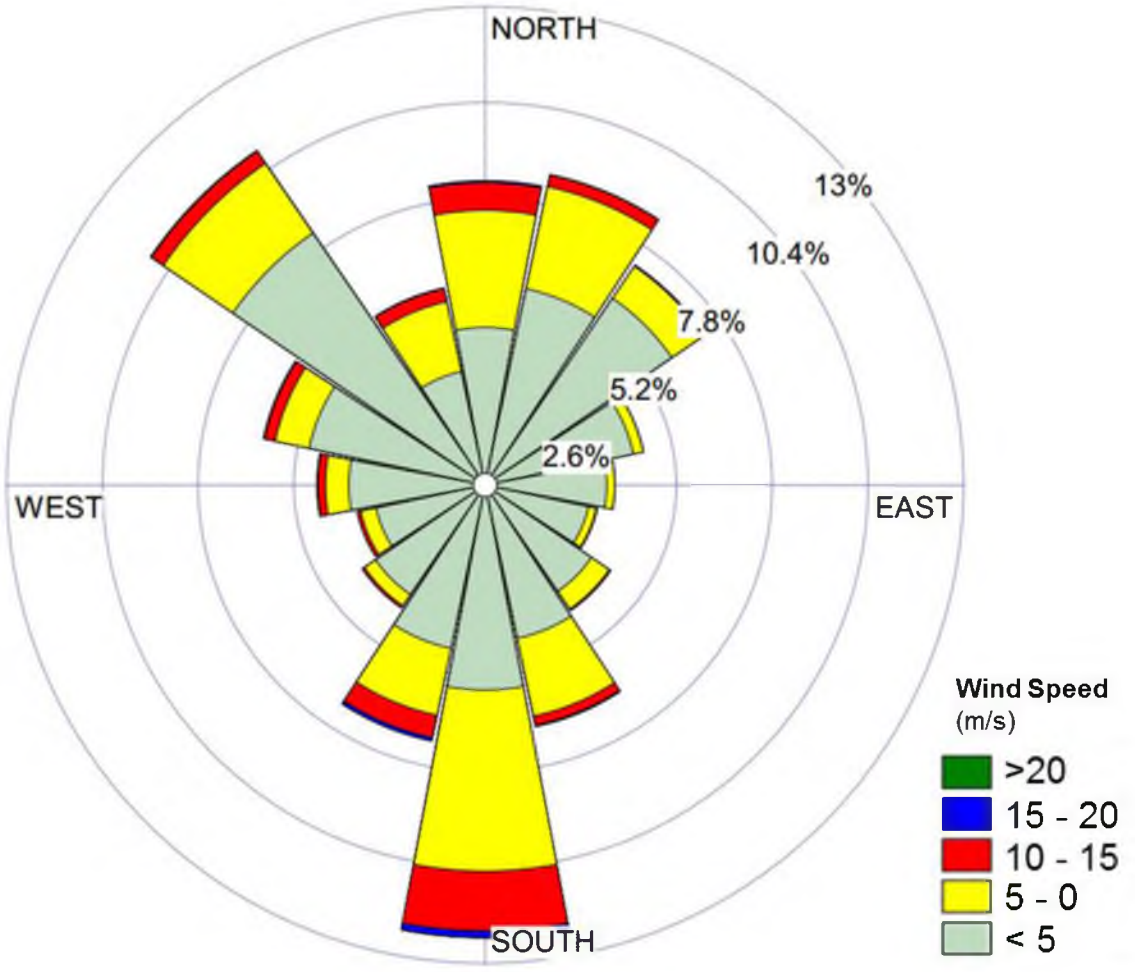

Figure 20. Wind data compiled for Callao, UT. Compiled data ranged from April 2000 – February 2014. Prevailing and dominant winds are from the south.

CONCLUSIONS

1. Reilly Wash Spit Complex (7.5×10^8 m^3) is a late transgressive depositional landform deposited during the ~10 kyr period prior to the Bonneville flood.
2. Tectonic geomorphic indices calculated for the Deep Creek Range, including mountain front sinuosity (Smf), valley floor width-to-height ratio (Vf), and hypsometric integral (HI), indicate Reilly Canyon Wash to be one of the least developed areas in the range in terms of watershed maturity. This immaturity, and subsequent state of dynamic equilibrium, are thought to have been caused by previously undocumented tectonic activity along watersheds 5-7 in the east central part of the range during the mid-late Quaternary (Figure 14 and 15). This activity resulted in the deposition of two large alluvial fans, which are not present anywhere else on the eastern flank of the Deep Creeks.
3. The alluvial fan at the base of Reilly Wash has been incised and eroded since the Quaternary, supplying sediment for the formation of a large spit-bar complex during the transgressive stage of Lake Bonneville (Gilbert, 1980; Hunt, 1981).
4. Orientation of the spit complex suggests that the dominant longshore drift direction was from the north, based on the north-south orientation of the complex and neighboring hook spit.

5. Estimated wind speeds were higher during the deposition of the RWSC than they are in present day. Winds were predominately from the north, unlike present day winds, which originate typically from the south.
6. Higher wind speeds and a large fetch (~ 100 kilometers) resulted in high wave energies acting on available sediments that led to the deposition of one of the largest landforms in the Lake Bonneville basin.
7. A sediment flux range of 1.2-1.5 x 10^4 m^3/yr was calculated based on the radiocarbon dates of gastropods samples C, E, G and the approximate age of the Bonneville Flood.
8. The radiocarbon ages (Table 1, F and G) obtained from two sites support the hypothesis of the U2 and U3 oscillations and their possible correlation to intermediate shorelines (Oviatt, 1997; Benson, 2011).

Future Work

This project is the first step in exploring intermediate shorelines in the western portion of the Bonneville basin. Higher resolution digital elevation models, coupled with ground penetrating radar, may result in a better understanding of the internal architecture of the spit complex, which would further clarify the depositional chronology. Additional exploration of the hook spit and tombolo, along with other Bonneville landforms along the Deep Creek Range, will increase our understanding of how the lake interacted along the western portion of the basin.

APPENDIX A

PHOTOS OF TUFA THIN SECTIONS AND OUTCROPS

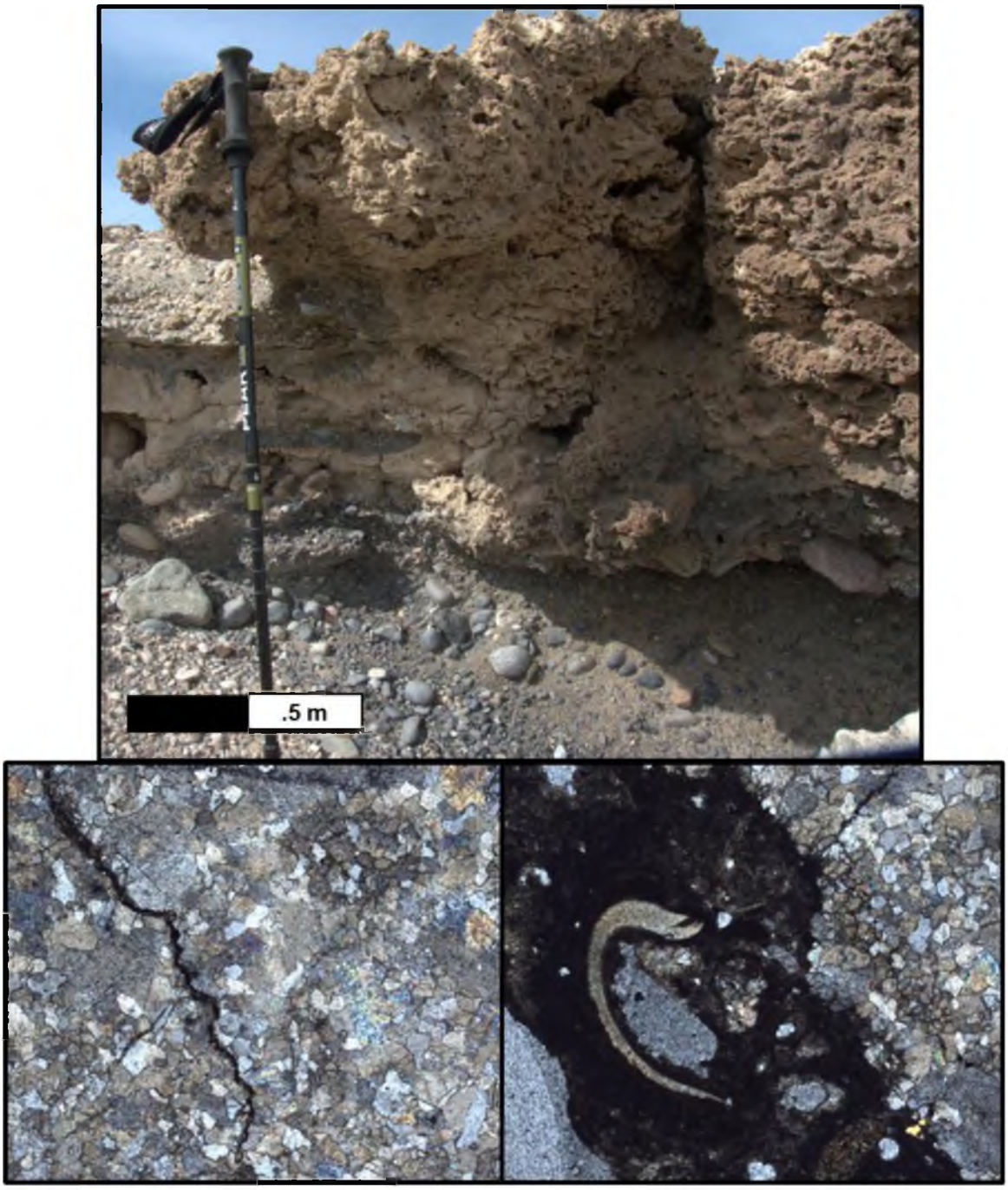

Figure 21. Tufa thin sections and outcrop photos (Knife Gully Upper). Top: Tufa located at the top of Knife Gully (Figure 5, location H). Bottom: Left) Stylolite Right). Dolomite clast with a gastropod shell imbedded among tufa.

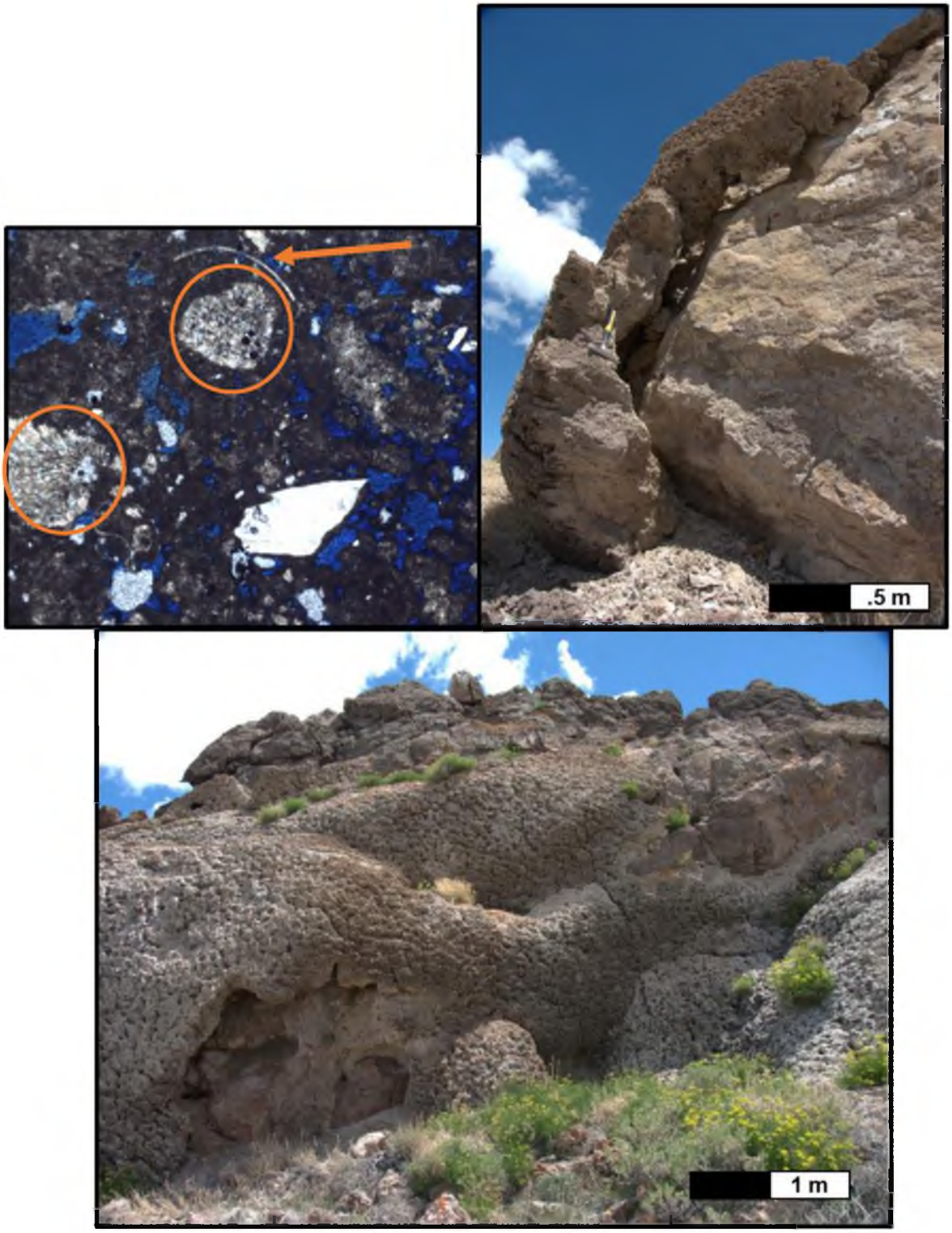

Figure 22. Tufa thin sections and outcrop photos (Tufa Tower). Capping tufa on Devonian aged dolomite (Figure 6, location 3). Top left: Thin section of capping tufa shown right and bottom with gastropod shell (arrow) and algae (circles).

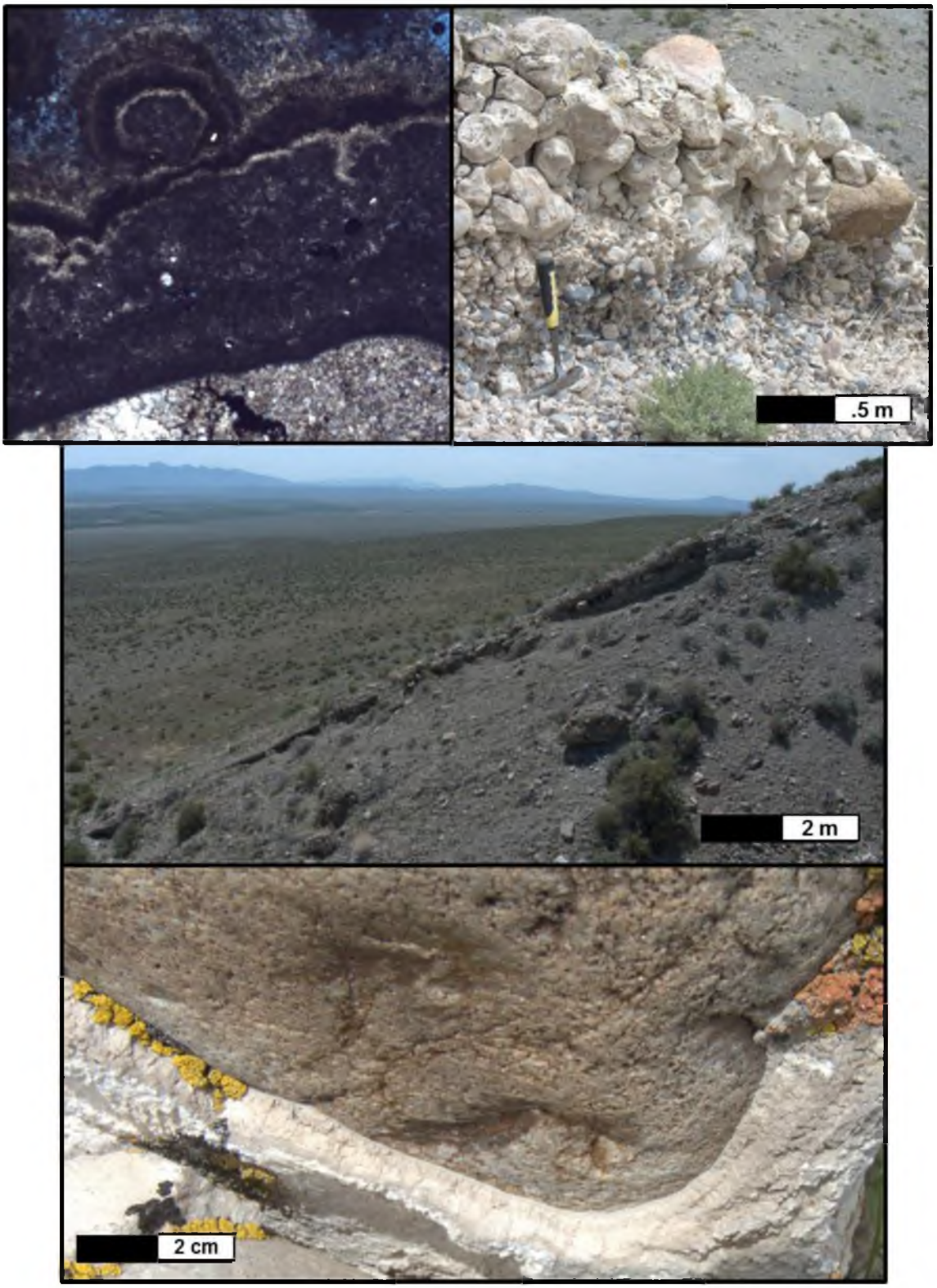

Figure 23. Tufa thin sections and outcrop photos (Incised Spit Complex Gully). Thin section (upper left) shows layering of tufa that cements the grains together. Outcrop photos show sample locations and bottom shows layering coating a quartzite cobble.

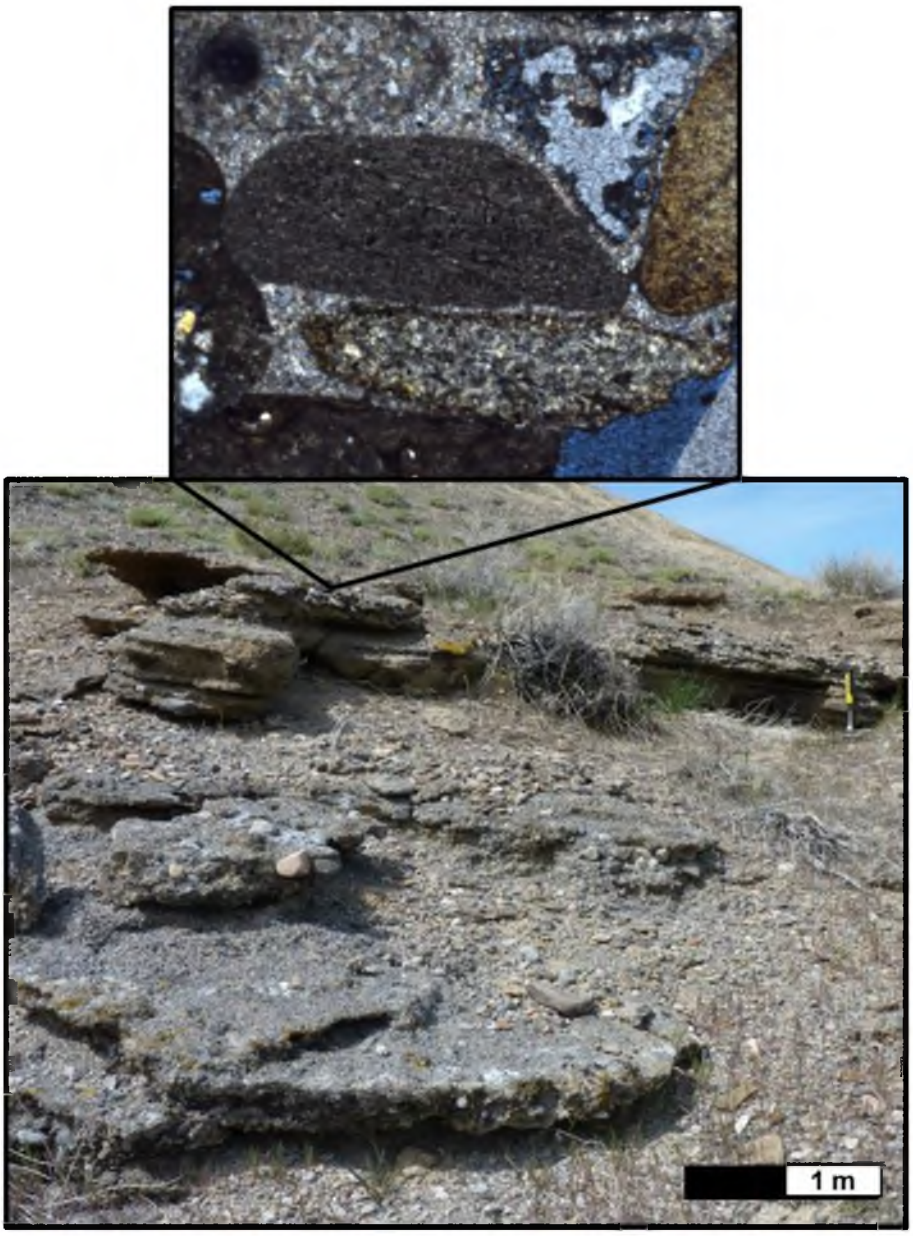

Figure 24. Tufa thin sections and outcrop photos (Reilly Wash Trench Site). Cemented beachrock at the base of Reilly Wash (Figure 6, location A; Figure 10). Thin section shows clasts with a calcium carbonate ($CaCO_3$) matrix.

APPENDIX B

HYPSOMETRIC CURVES

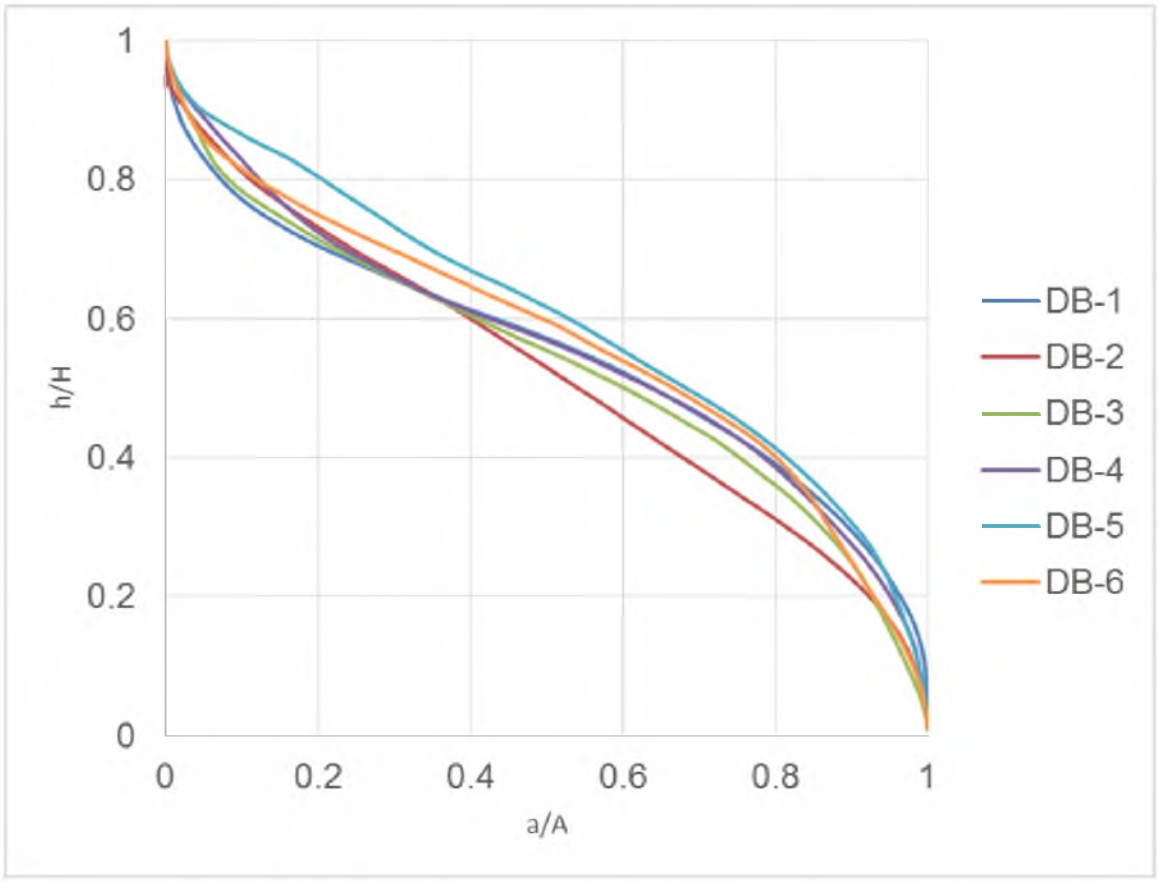

Figure 25. Plotted hypsometric curves. For drainage basin (DB) locations, refer to Figure 15.

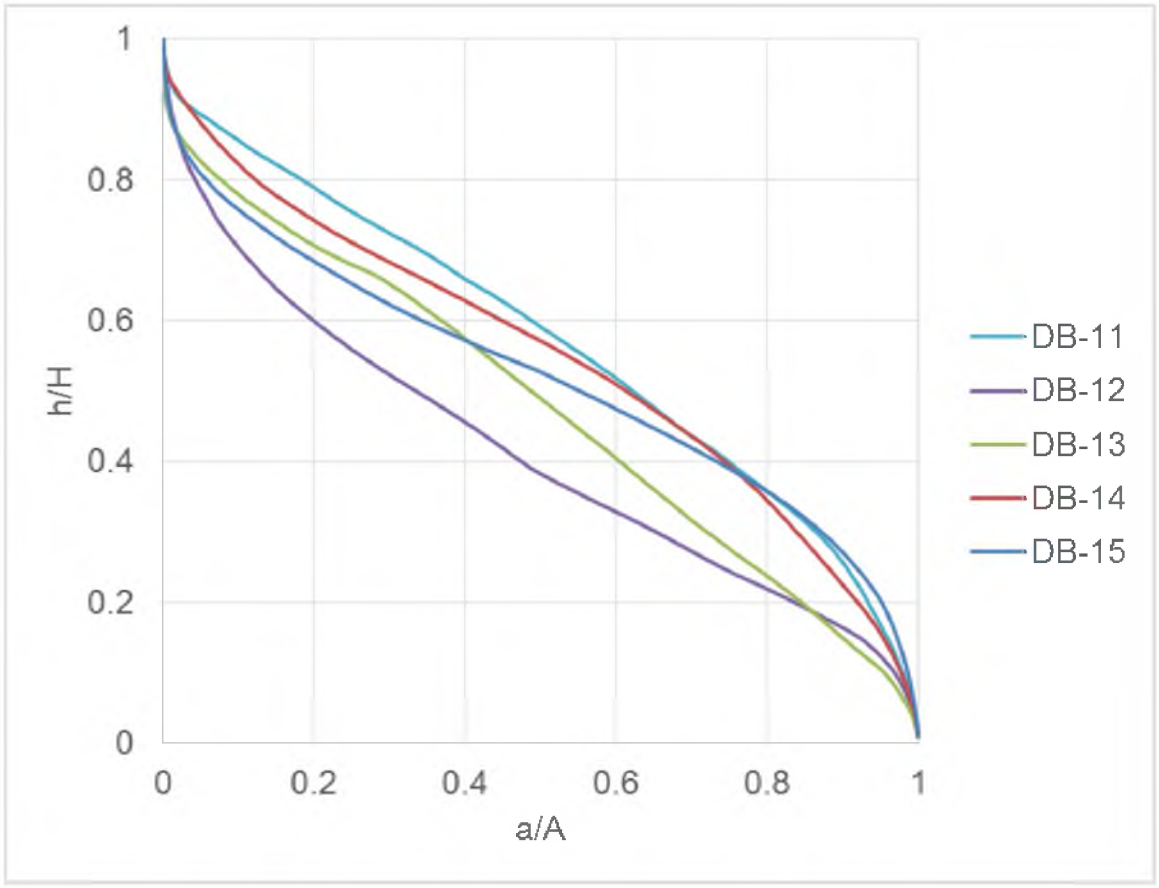

Figure 25 (continued).

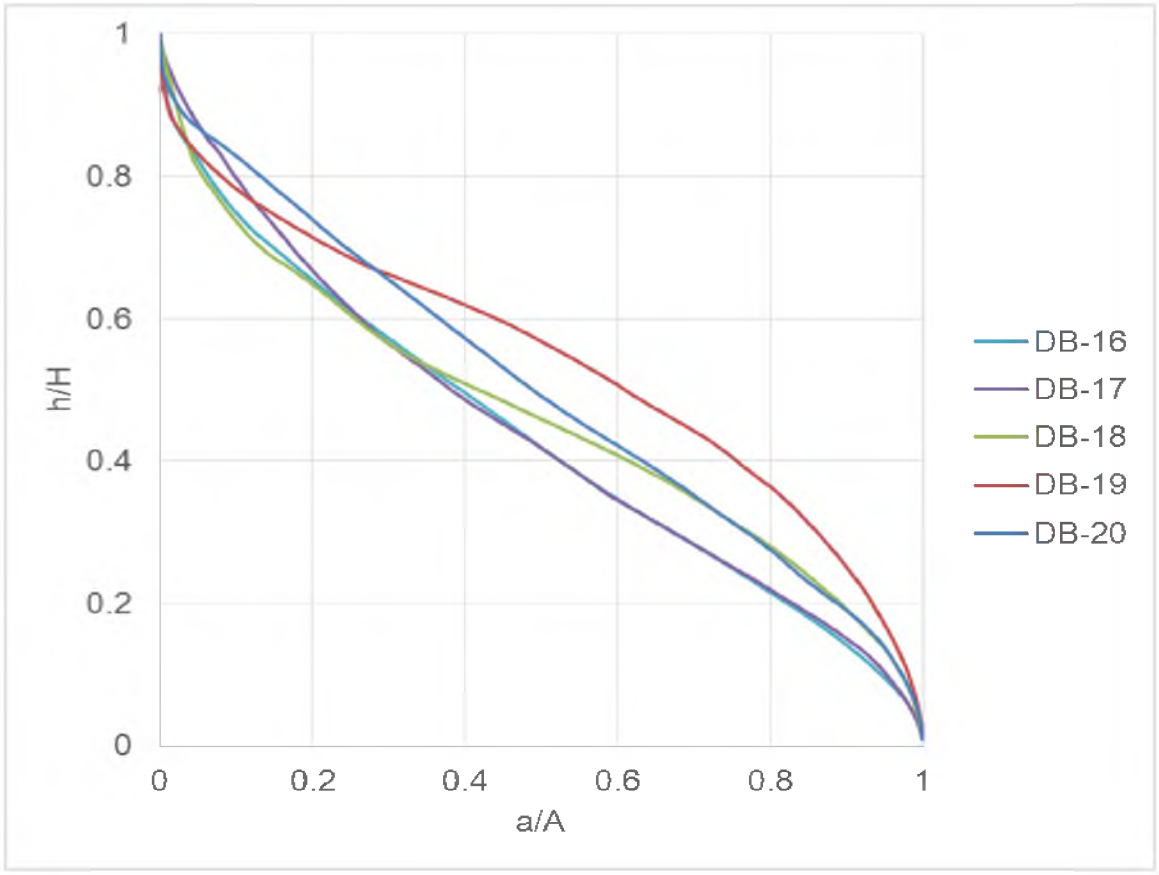

Figure 25 (continued).

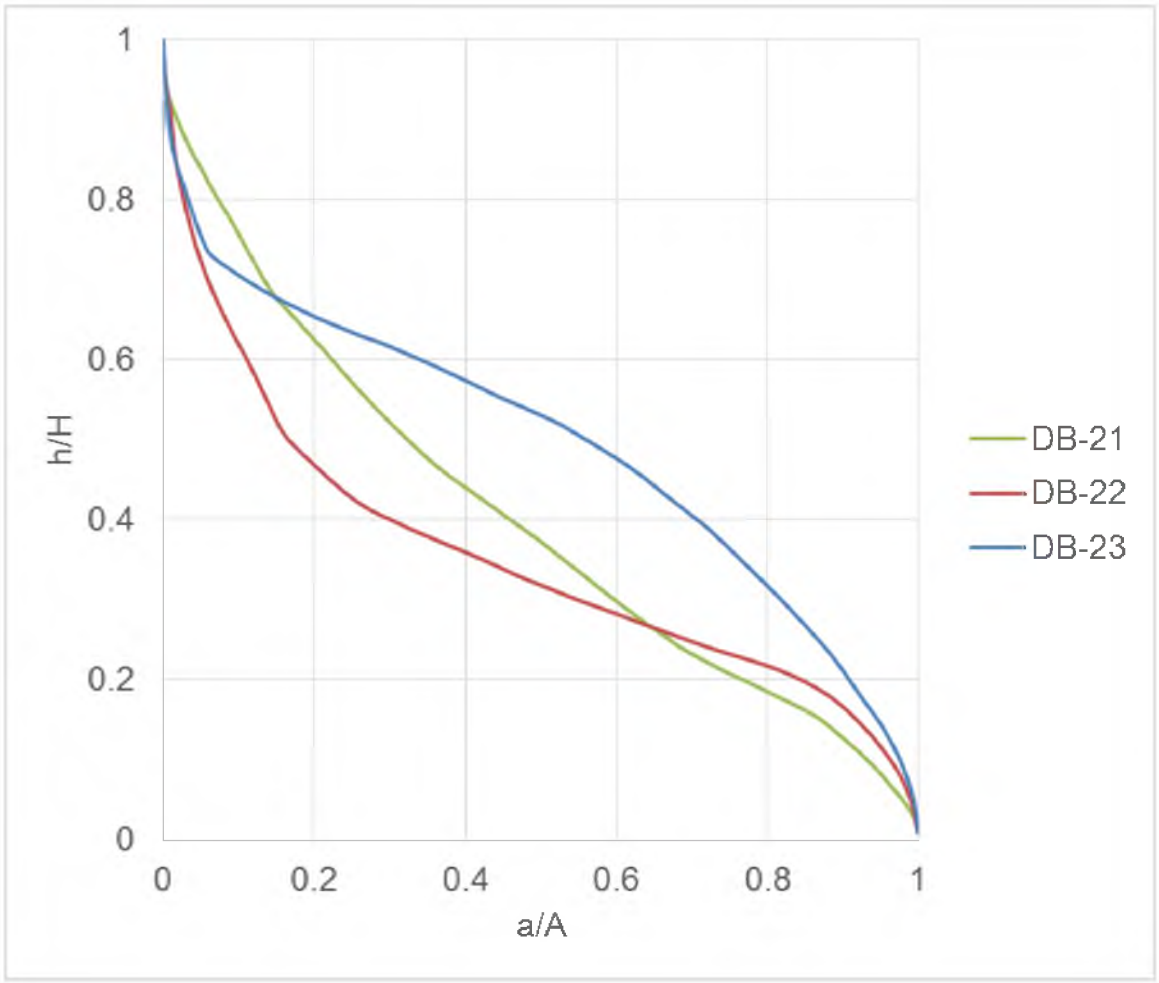

Figure 25 (continued).

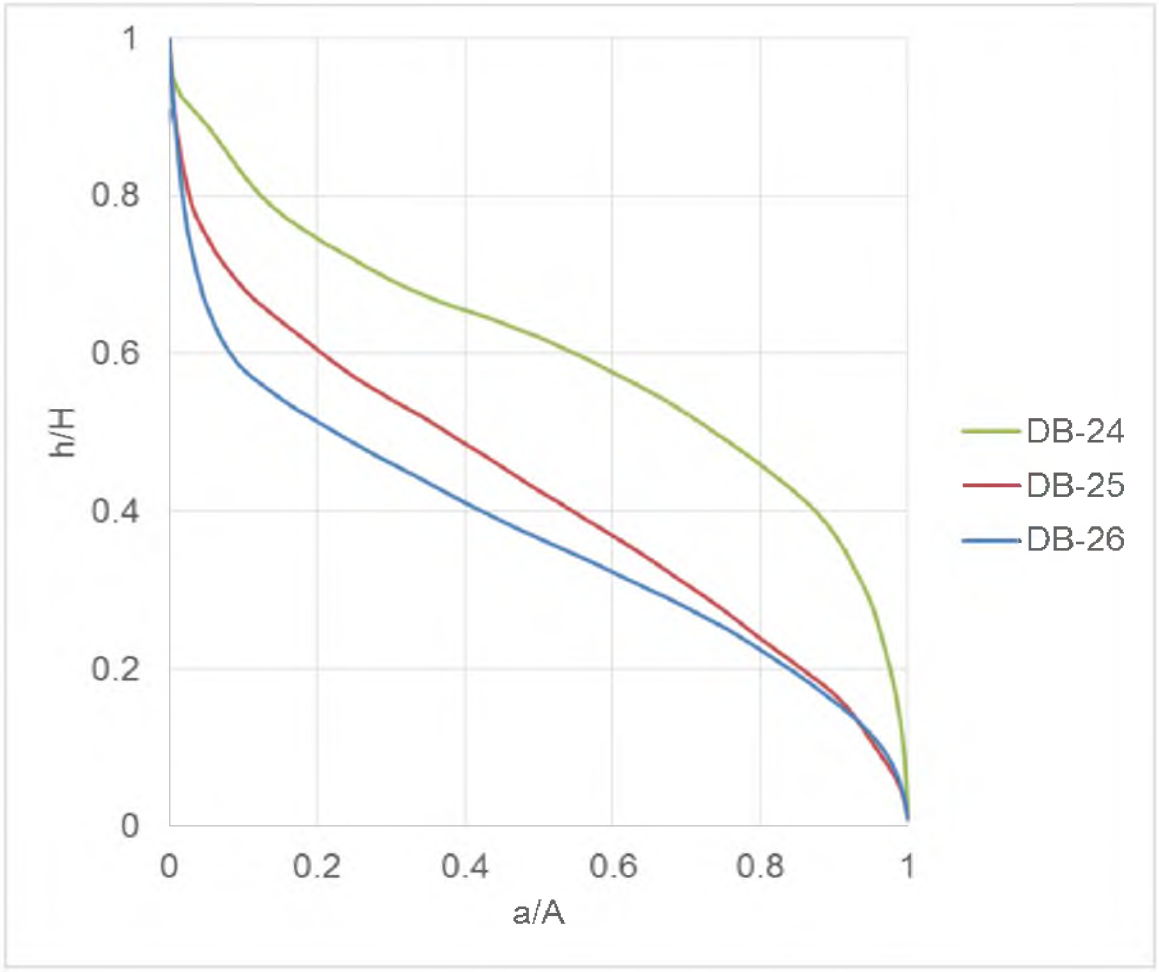

Figure 25 (continued).

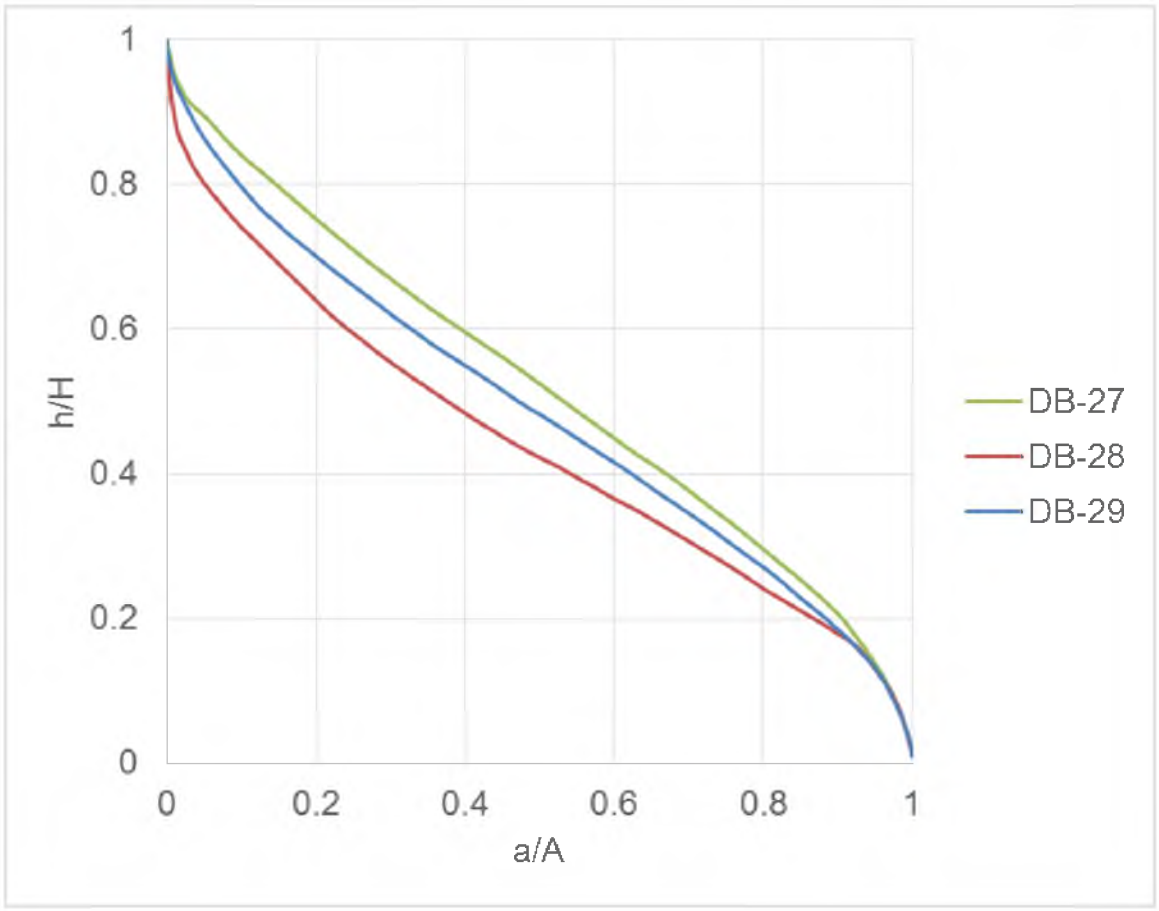

Figure 25 (continued).

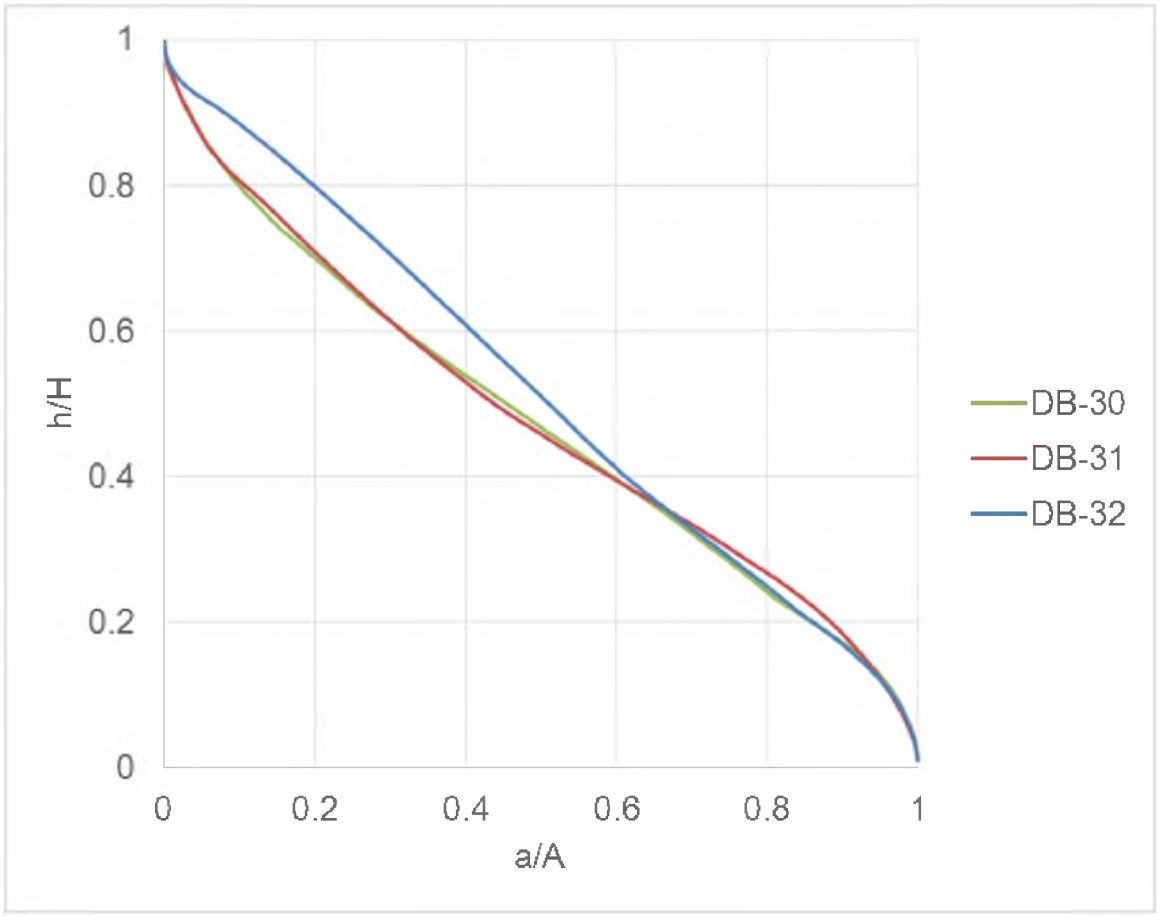

Figure 25 (continued).

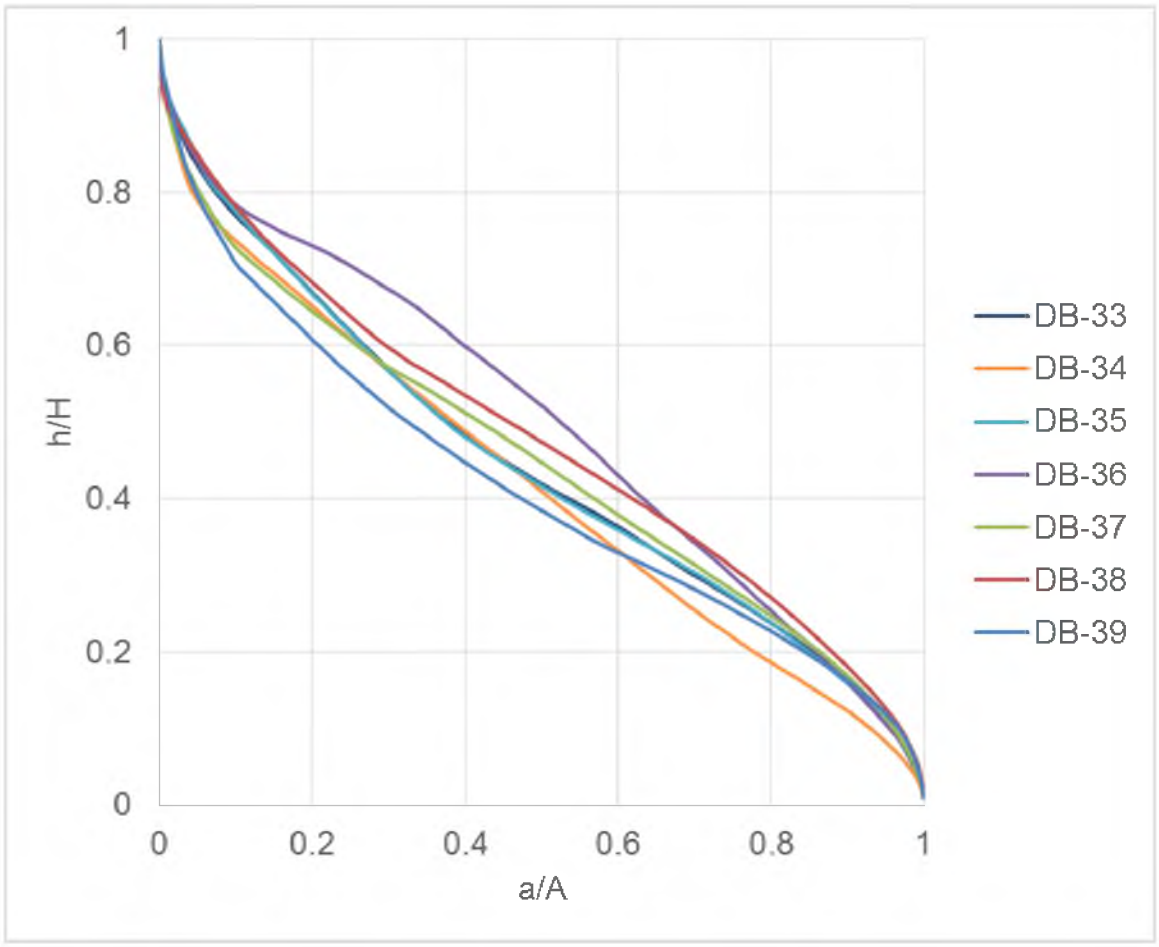

Figure 25 (continued).

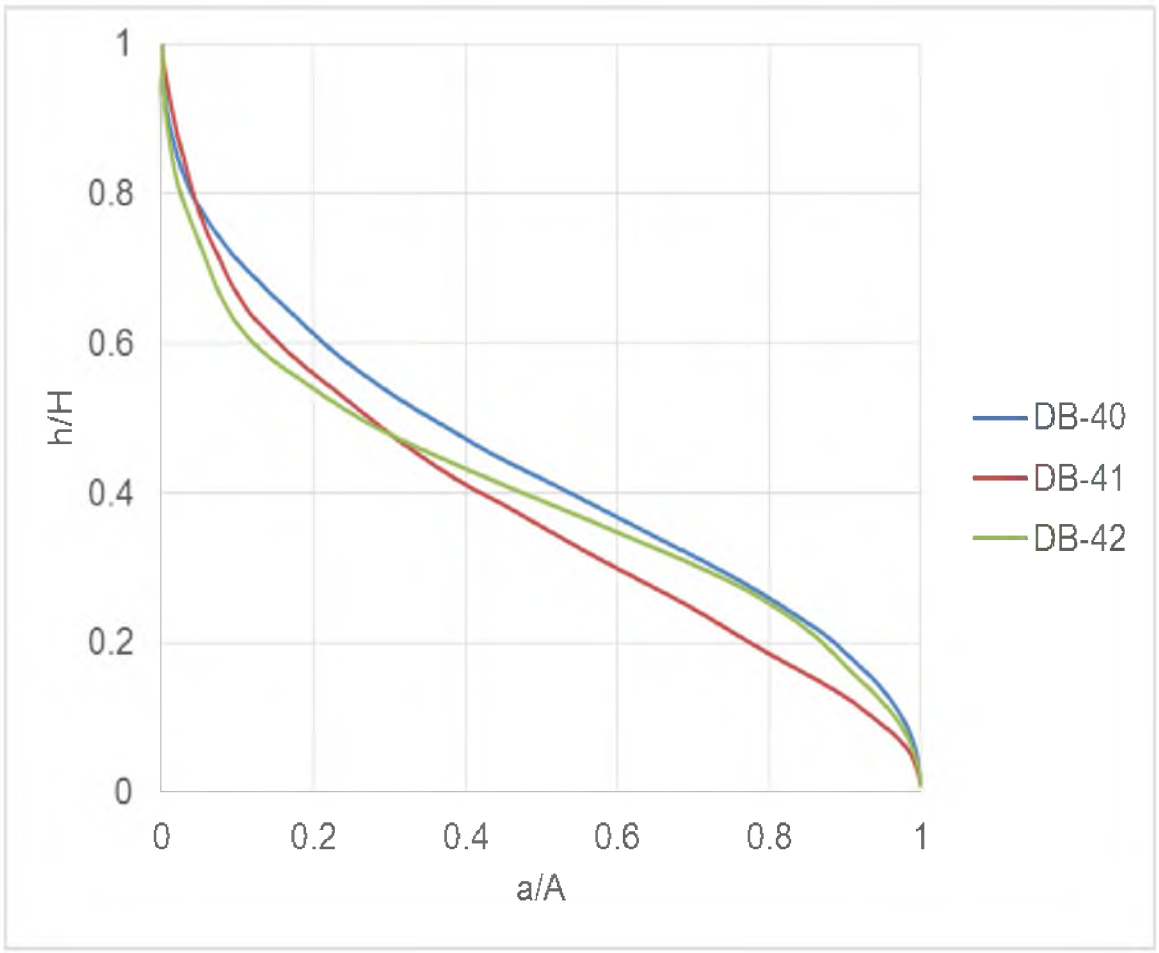

Figure 25 (continued).

REFERENCES

Adams, K.D., 2003. Estimating palaeowind strength from beach deposits. Sedimentology, 50, 565–577.

Adams, K.D., 2004. Estimating palaeowind strength from beach deposits - Reply. Sedimentology, 51, 671–673.

Adams, K.D., Wesnousky, S.G., 1998. Shoreline processes and the age of the Lake Lahontan highstand in the Jessup embayment, Nevada. Geological Society of America. Bulletin 110, 1318-1332.

Benson L.V., Currey D.R., Dorn R.I., Lajoie K.R., Oviatt C.G., Robinson S.W., Smith G.I., Stine S. 1990. Chronology of expansion and contraction of four Great Basin lake systems during the past 35,000 years. Palaeogeography, Palaeoclimatology, Palaeoecology 78, 241–286.

Benson, L.V., Lund, S.P., Smoot, J.P., Rhode, D.E., Spencer, R.J., Verosub, K.L., Louderback, L.A., Johnson, C.A. Rye, R.O., Negrini, R.M., 2011. The rise and fall of Lake Bonneville between 45 and 10.5 ka. Quaternary International 235, 57-69.

Bick, K.F., 1966. Geology of the Deep Creek Mountains, Tooele and Juab Counties, Utah. Utah Geological and Mineralogical Survey Bulletin 77, 120 p.

Bull, W.B., 1984. Tectonic geomorphology. Journal of Geological Education 32, 310–324.

Bull, W.B. 2007. Tectonic Geomorphology of Mountains. Blackwell Publishing Ltd, 117-164.

Bull, W.B., McFadden, L.D., 1977. Tectonic geomorphology north and south of the Garlock fault, California. In: Doehring, D.C. (Ed.), Geomorphology in Arid Regions, Proceedings 8th Annual Geomorphology Symposium. State University of New York, Binghamton, NY, pp. 115–137.

Bunte, K., Abt, S.R., 2001. Sampling surface and subsurface particle-size distributions in wadable gravel- and cobble-bed streams for analyses in sediment transport, hydraulics, and streambed monitoring. Gen. Tech. Rep. RMRS-GTR-74. Fort Collins, CO: U.S. Department of Agriculture, Forest Service, Rocky Mountain Research Station. 428 p.

Burr, T.N., Currey, D.R., 1992. Linear model of threshold-controlled paleoshorelines of Lake Bonneville. In: Machette, M.N., Currey, D.R. (Eds.), In the footsteps of G.K. Gilbert, Lake Bonneville and Neotectonics of the Eastern Basin and Range Province. Utah Geological and Mineral Survey Miscellaneous Publication, 88-1, 104-110.

CERC, 1984. Shore Protection Manual. US Army Corps of Engineers, Waterway Experiment Station, Coastal Engineering Research Center, Volumes I and II, Superintendent of Documents, Washington, D.C.

Clifton, H.E., Dingler, J.R., 1984. Wave-formed structures and paleoenvironmental reconstruction. Marine Geology 60, 165-198.

Currey, D.R., Oviatt, C.G., 1985. Durations, average rates, and probable causes of Lake Bonneville expansions, stillstands, and contractions during the last deep-lake cycle, 32,000 to 10,000 yrs ago. Geological Journal of Korea 10, 1085-1099.

Evans, O.F., 1942. The origin of spits, bars, and related structures. Journal of Geology 50, 846–965.

Felton, A., Jewell, P.W., Chan, M., Currey, D., 2006. Controls of tufa development in Pleistocene Lake Bonneville, Utah. Journal of Geology, 114, 377-389.

Font, M., Amorese, D., Lagarde, J.-L., 2010. DEM and GIS analysis of the stream gradient index to evaluate effects of tectonics: the Normandy intraplate area (NW France). Geomorphology 119, 172–180.

Forester, R.M., 1988. Nonmarine calcareous microfossil sample preparation and data acquisition procedures. U.S. Geological Survey Technical Procedure HP-78, R2, 1-9.

Gilbert, G.K., 1890. Lake Bonneville. U.S. Geological Survey Monograph 1, 438 p.

Godsey, H.S., Currey, D.R., Chan, M.A., 2005. New evidence for an extended occupation of the Provo paleoshoreline and implications for regional climate change, Pleistocene Lake Bonneville, Utah, USA. Quaternary Research 63, 212-223.

Godsey, H.S., Oviatt, C.G., Miller, D.M., Chan, M.A., 2011. Stratigraphy and chronology of offshore to near shore deposits associated with the Provo shoreline, Pleistocene Lake Bonneville, Utah. Palaeogeography, Palaeoclimatology, Palaeoecology 310, 442-450.

Gregory, M., Chan, M., Currey, D., Schofield, I., 2006. Transgressive landforms and lithofacies models of Pleistocene Lake Bonneville, Utah in Geology of northwest Utah. In: Harty, K.M., Tabet, D.E. (Eds.), Utah Geological Association Publication, p. 34.

Hack, J.T., 1973. Stream profile analysis and stream-gradient index. Journal Res. United States Geological Survey 1, 421– 429.

Hintze, L.F., Willis, G.C., Laes, D.Y.M., Sprinkel, D.A., Brown, K.D., 2000. Digital geologic map of Utah: Utah Geological Survey Map 179DM, 17 p., scale 1:500,000.

Hunt, C.B., 1981. Pleistocene Lake Bonneville, ancestral Great Salt Lake, as described in the notebooks of G.K. Gilbert, 1875–1880. Brigham Young University Geological Studies 29, part 1, 231 p.

Janecke, S.U., Oaks, R.Q., 2011. New insights into the outlet conditions of late Pleistocene Lake Bonneville, southeastern Idaho, USA. Geosphere 7, 1369-1391.

Jewell, P.W., 2007. Morphology and paleoclimatic significance of Pleistocene Lake Bonneville spits. Quaternary Research 68, 421-430.

Johnson, J.W., 1956. Dynamics of nearshore sediment movement. American Association of Petroleum Geologists Bulletin, 40 (9), 2211-2232.

Keller, E.A., Pinter, N., 2001. Active tectonics: Earthquakes, uplift, and landscape. Upper Saddle River, NJ, Prentice Hall, 362 p.

Komar, P.D., 1998. Beach processes and sedimentation. Upper Saddle River, NJ, Prentice Hall, 543 p.

Krist Jr, F., Schaetzl, R.J., 2001. Paleowind (11,000 BP) directions derived from lake spits in Northern Michigan. Geomorphology, 38 (1-2), 1-18.

Malde, H.E., 1968. The catastrophic late Pleistocene Bonneville flood in the Snake River Plain, Idaho, U.S. Geological Survey Professional Paper 596, 52 p.

Munsell Color, 1991. Munsell Soil Color Charts. Revised Edition. Newburgh, New York, Macbeth, Division of Kollmorgen Instruments Corp.

O'Connor, J.E., 1993. Hydrology, hydraulics and geomorphology of the Bonneville flood. Geological Society of America Special Paper 274, 83 pp.

O'Connor, J.E., Costa, J.E., 2004. The World's largest floods, past and present-Their causes and magnitudes. U.S. Geological Survey Circular 1254, 13 p.

Orme, A.J., Orme, A.R., 1991. Relict barrier beaches as paleoenvironmental indicators in the California desert. Physical Geography 12, 334–346.

Oviatt, C.G., 1997. Lake Bonneville fluctuations and global climate change. Geology 25, 155-158.

Oviatt, C.G., Currey, D.D., Miller, D.M., 1990. Age and paleoclimatic significance of the Stansbury Shoreline of Lake Bonneville, northeastern Great Basin. Quaternary Research 33, 291-305.

Oviatt, C.G., Currey, D.R., Sack, D., 1992. Radiocarbon chronology of Lake Bonneville, Eastern Great Basin, USA. Palaeogeography, Palaeoclimatology, Palaeoecology 99, 225-241.

Oviatt, C.G., Madsen, D.M., Schmitt, D.N., 2003. Late Pleistocene and Early Holocene rivers and wetlands in the Bonneville basin of western North America. Quaternary Research 60, 200-210.

Oviatt, C.G., Miller, D.M., McGeehin, J.P., Zachary, C., Mahan, S., 2005. The Younger Dryas phase of Great Salt Lake, Utah, USA. Palaeogeography, Palaeoclimatology, Palaeoecology 219, 263-284.

Pérez-Peña, J.V., Azañón, J.M., Booth-Rea, G., Azor, A., Delgado, J., 2009c. Differentiating geology and tectonics using a spatial autocorrelation technique for the hypsometric integral. Journal of Geophysical Research 114, 1–15.

Pérez-Peña, J.V., Azor, A., Azañón, J.M., Keller, E.A., 2010. Active tectonics in the Sierra Nevada (Betic Cordillera, SE Spain): Insights from geomorphic indexes and drainage pattern analysis. Geomorphology 119, 74–87.

Rodgers, D.W., 1989. Geologic map of the Deep Creek Mountains Wilderness Study Areas, Tooele and Juab Counties, Utah: U.S. Geological Survey Miscellaneous Field Studies Map MF–2099, scale 1:50,000.

Schofield, I., Jewell, P.W., Chan, M., Currey, D.R., Gregory, M., 2004, Shoreline development, longshore transport and surface wave dynamics, Pleistocene Lake Bonneville, Utah. Earth Surface Processes and Landforms, 29, 675-1690.

Silva, P.G., Goy, J.L., Somoza, L., Zazo, C., Bardají, T., 1993. Landscape response to strike–slip faulting linked to collisional settings: Quaternary tectonics and basin formation in the Eastern Betics, southeastern Spain. Tectonophysics 224, 289–303.

Strahler, A.N., 1952. Hypsometric (area–altitude) analysis of erosional topography. Geological Society of America Bulletin 63, 1117–1142.

Stuiver, M., Reimer, P.J., Bard, E., Beck, J.W., Burr, G.S., Hughen, K.A., Kromer, B., McCormac, G., van der Plicht, J., Spurk, M., 1998. INTCAL98 Radiocarbon Age Calibration, 24000-0 cal BP. Radiocarbon 40(3), 1041-1083.

Thomson, K.C., 1973. Mineral deposits of the Deep Creek Mountains, Tooele and Juab Counties, Utah. Utah Gelogical and Mineralogical Bulletin 99, 120 p.

Wolman, M.G., 1954. A method of sampling coarse river-bed material: Transactions of the American Geophysical Union, 35, 951-956.

Zovoili, E., Konstantinidi, E., Koukouvelas, I.K., 2004. Tectonic geomorphology of escarpments: The cases of Kompotades and Nea Anchialos faults. Bulletin of the Geological Society of Greece, XXXVI, 1716-1725.